IMPERMEABLE BOREHOLES FOR HIGH TEMPERATURE THERMAL ENERGY STORAGE

REPORT 2020:666

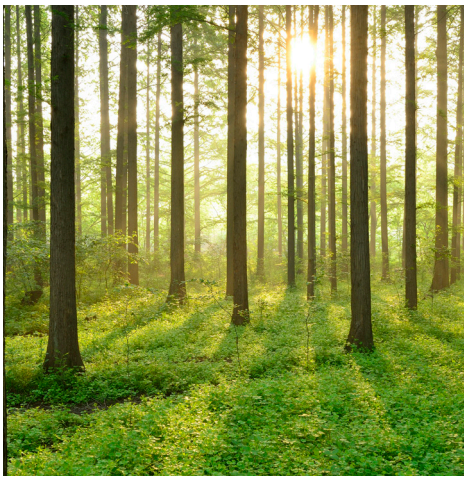

TERMISKA ENERGILAGER

Energiforsk

Impermeable Boreholes for High Temperature Thermal Energy Storage

MAX HESSELBRANDT, JOSÉ ACUÑA AND JOHAN FUNEHAG

ISBN 978-91-7673-666-1 | © Energiforsk April 2020

Energiforsk AB | Phone: 08-677 25 30 | E-mail: kontakt@energiforsk.se | www.energiforsk.se

Förord

Lagring av höggradig värme över säsonger är eftersträvansvärt för flera energibolag. Inte minst de som sommartid har en outnyttjad värmeresurs och vintertid har dyrare produktion att ersätta. Borrhålslager är i flera avseenden attraktiva för att fylla denna funktion men det finns utvecklingsbehov, bland annat av kostnadseffektiva kollektorlösningar anpassade till högre temperaturer. Projektet har undersökt öppna, tryckbärande borrhål med en koaxial kollektorkonfiguration anpassad till temperaturnivåer upp mot 100 °C.

Projektet Tryckbärande borrhål för högtemperaturlager har genomförts av ett projekt-team lett av José Acuña, Bengt Dahlgren. Projektet har finansierats av, och ingår i, Energiforsks program Termiska Energilager. Ett forskning- och utvecklingsprogram vars långsiktiga mål är att visa hur, var och när termiska energilager kan utformas och användas och vilken ekonomisk och miljömässig nytta de kan ge.

En fokusgrupp bestående av Henrik Lindståhl (Tekniska verken i Linköping AB), Morgan Romvall (Halmstad Energi och Miljö AB), Lennart Hjalmarsson (Göteborg Energi AB) och Mutaz Alkiswani (Öresundskraft Kraft & Värme AB) har följt och kvalitetssäkrat projektet.

Programmet Termiska lager leds av en styrgrupp bestående av Henrik Lindståhl (ordförande) (Tekniska verken i Linköping AB), Lennart Hjalmarsson (Göteborg Energi AB), Per Haker (Hässleholm Miljö AB), Einar Port (Mälarenergi AB), Per Kallner (Vattenfall R&D AB), Mutaz Alkiswani (Öresundskraft Kraft & Värme AB), Joacim Cederwall, (Jönköping Energi AB), Morgan Romvall (Halmstad Energi och Miljö AB), Ted Edén (Norrenergi AB), Fredrik Martinsson, Markus Wråke och Julia Kuylenstierna (adjungerade Energiforsk). Suppleanter har bestått av Ulf Hagman (Göteborg Energi), Marianne Allmyr, (Mälarenergi AB), Mile Elez (Tekniska verken i Linköping AB), Jesper Baaring (Öresundskraft Kraft & Värme AB), Mats Svensson (Halmstad Energi och Miljö AB), Staffan Stymne (Norrenergi AB), Patric Jönnervik (Jönköping Energi AB) och Erik Holmén (ENA Energi).

Stockholm, april 2020

Julia Kuylenstierna

Programansvarig Energiforsk

These are the results and conclusions of a project, which is part of a research programme run by Energiforsk. The author/authors are responsible for the content.

Författarens förord

Detta projekt blev en resa genom befintlig och ny kunskap, tillsammans med en projektgrupp som successivt omvandlades i takt med att forskningsfrågan och arbetsmetodiken i projektet blev närmare definierat.

Jag skulle vilja tacka några få personer som vid något tillfälle gjorde ett avgörande bidrag: Tony Jernström (Geobatteri AB), Stefan Swartling (Wassara), Johan Olovsson (BESAB) och Mikael Erlström (SGU). Era bidrag blev milstolpar i projektet!

Vi har tillsammans lyckats få ett bättre förståelse på hur grundvattnet kan strömma i geoenergiborrhål via sprickor och visat via avancerad injektering av lämpligt material att sprickorna kan tätas på ett kontrollerat sätt, dvs ett Tryckbärande Borrhål i ett borrhålslager är praktiskt möjligt, trots att det kräver omfattande insatser.

Tack till samtliga företag som finansierade denna forskning, och tack Fredrik Martinsson och Julia Kuylenstierna som på Energiforsk har lett forskningsprogrammet Termiska Energilager på ett ypperligt sätt.

Vi ses i nästa projekt!

José Acuña
Projektledare

Sammanfattning

Den termiska prestandan hos ett borrhålsvärmelager är till stor del beroende av utformningen av de borrhålsvärmeväxlare som utnyttjas för värmeväxling mellan värmebärare och berg. För att möjliggöra inlagring och urladdning av värme vid höga temperaturer så krävs utveckling av nya temperaturbeständiga kollektorlösningar som dessutom uppfyller de krav som ställs på hydraulisk och termisk prestanda.

Detta pilotprojekt utfördes i syfte att undersöka möjligheten till att tillämpa injektering som en tätande åtgärd för att reducera eller förhindra utläckage av vatten i öppna, tryckbärande borrhål. Projektet är ämnat som ett första steg i utvecklingen av en koaxial borrhålsvärmeväxlare avsedd för högtemperaturlagring i hårt berg.

Projektet har behandlat hur samspelet mellan bergets hydrogeologiska egenskaper, injekteringsmedlets egenskaper och utförandet av en eventuell injekteringsinsats påverkar borrhålsväggens täthet. En designmetodik och procedur har utvecklats för genomförande av injektering samt efterföljande hydrauliska mätningar i avskärmade borrhålssektioner. Målet var att framställa en metod så att sektionen kan injekteras, öppnas samt trycksättas kort efter injektering utan risk för negativ påverkan på tätningen.

Fältförsök har utförts i syfte att testa metoden under praktiska förhållanden. Dessa föregicks av förundersökningar för kartläggning av de geologiska och hydrogeologiska förhållandena på platsen, vilka utgjorde underlag för planering och design inför fältinjekteringen. Sammantaget visar resultaten att tätning av sprickor med både cement och fintätningsmedel (silica sol) samt efterföljande hydrauliskt test kort efter injektering har kunnat utföras enligt det förfarande som utvecklats inom ramen för projektet. Flera försök kunde genomföras utan att påverkan på tätningseffekten kunde påvisas. I framtiden kan metoden utvecklas för att möjliggöra en snabb och effektiv process för utförande och kontroll av de tätande åtgärderna, till exempel i samband med borrning.

Potentialen i att tillämpa injektering som en aktiv metod för att producera borrhålsvärmeväxlare avsedda för högtemperaturlager är avhängig på de generella täthetskrav som föreligger för att tillgodose erforderlig hydraulisk prestanda i systemet. Det kan konstateras att förutsättningar finns för att uppnå mycket låg genomsläpplighet genom fintätning med icke cementbaserade injekteringsmedel så som silica sol. Frågan kring vilken täthetsgrad som fordras givet specifika förutsättningar har inte omfattats av detta projekt och bör därför utredas i framtiden. Detta är av stor betydelse vad gäller omfattningen av de tätningsinsatser som krävs, och är således avgörande för bedömning av ekonomisk samt teknisk genomförbarhet för storskalig produktion.

För en mer omfattande svensk sammanfattning, se Energiforsk rapport 2020:667 *Tryckbärande borrhål för högtemperaturlager.*

Summary

The thermal performance of a borehole thermal energy storage is highly dependent on the design of the heat exchangers used to provide heat exchange between the heat carrier and the rock. Development of new temperature-resistant borehole heat exchanger designs is an important step in accomplishing efficient storage of industrial surplus heat at high temperatures.

This pilot study has focused on investigating the application of permeation grouting techniques as a possible means of preventing or reducing fluid losses in open-hole pressurized boreholes. The study is intented as a first step in the development of a novel type of coaxial borehole heat exchanger for high temperature borehole thermal energy storage applications in hard rock.

The study has dealt with the interaction of parameters affecting the tightness of the borehole wall after grouting, including hydrogeological characteristics of the rock mass, grout material properties and grouting performance. A design methodology and approach for grouting and post-grouting hydraulic testing in packed-off borehole sections has been developed. The aim was to provide a method that allows for grouting, re-opening and immidiate post-grouting hydraulic testing of the borehole section without risking impairing the sealing effect achieved by the grouting effort.

Grouting field experiments aiming to demonstrate the proposed procedure under practical conditions have been carried out. Pre-investigations were performed for characterization of the undisturbed rock mass prior to the grouting field experiments. The results show that grouting using both cement-based grouts and fine-sealing agents (silica sol) as well as post-grouting hydraulic testing could be performed in accordance with the proposed procedure. Several attempts were performed without observing decreased sealing effect during post-grouting hydraulic testing. Future development can be made for enabling fast and efficient implementation and sealing performance verification of the grouting efforts, for example in connection with drilling advancement.

Concerning the use of permeation grouting techniques as an active method for implementating BHE fields for HT-BTES applications, the feasibility is highly dependent on those tightness requirements that must be met to ensure adequate hydraulic performance of the system. It can be concluded that very high levels of sealing can be achieved using fine sealing agents such as silica sol. However, the question of what levels of tightness are needed under given specific conditions is still open and should therefore be investigated in future research. This is an important consideration concerning the extent of efforts required, thus crucial for assessments of economic and technical feasibility of large-scale implementations.

List of content

1 Introduction 9

1.1 Background 9

1.2 Scope and methodology of study 11

2 Literature review 13

2.1 Hard rock hydrogeology 13

2.2 Permeation grouting in hard rock 16

2.2.1 Properties of grout materials 16

2.2.2 Grout penetration 18

2.2.3 Mechanical breakdown of fresh grout 19

2.3 Drilling techniques for shallow geothermal energy systems 20

3 Pre-investigations and hydrogeological characterization 22

3.1 Site description and borehole directional surveys 22

3.2 Wire-line geophysical logging 24

3.3 Hydraulic testing 26

3.4 Thermal testing 28

3.5 Summary of borehole investigations 28

3.6 Estimation of fracture transmissivity distributions 33

4 Grouting design methodology 36

4.1 General description of grouting and hydraulic testing procedure 36

4.2 Tightness Conditions and requirements 37

4.3 Grouting design based on penetration length and material strength development 37

4.3.1 Penetration length 38

4.3.2 Stop criteria 39

4.4 Detailed description of grouting and hydraulic testing procedure 41

5 Grouting field experiments 43

5.1 Equipment and materials 43

5.1.1 Grouting equipment 43

5.1.2 Inhole equipment 43

5.1.3 Hydraulic testing equipment 43

5.1.4 Grouting materials and grout properties testing equipment 44

5.2 Implementation 45

5.2.1 Cement grouting 47

5.2.2 Silica sol grouting 47

5.3 Future field work 48

6 Results 49

6.1 Grouted test sections 50

6.2 Non-grouted test sections 51

6.3 Overall borehole tightness 54

7	**Discussion**	**56**
8	**Summary, conclusion and future work**	**60**
9	**References**	**62**

1 Introduction

1.1 BACKGROUND

Waste heat is an inevitable by-product of every energy conversion process. Estimations show that around 50% of the global production of primary energy is wasted as exhaust or effluent losses, out of which approximately 60% are generated at temperature levels below 100 °C (Forman et al. 2016). Indeed, waste heat recovery has been recognized as a means to improve overall energy efficiency and reduce greenhouse gas emissions (U.S. Department of Energy 2008; Cabeza 2015).

Borehole thermal energy storage (BTES) or more specifically high temperature BTES (HT-BTES), appears to be a promising approach for large-scale, long-term, sensible thermal storage of excess heat from solar thermal collectors, cogeneration plants or other industrial processes (Welsch et al. 2018; Gehlin 2016; Reuss 2015). BTES systems make use of the ground as storage medium, in which vertical borehole heat exchangers (BHEs) are densely inserted. A heat transfer fluid is circulated through the BHE network and exchanges heat with the surrounding ground mainly by conduction. Various loop-configurations exist, including single or multiple U-tube and coaxial BHE configurations, see Figure 1-1.

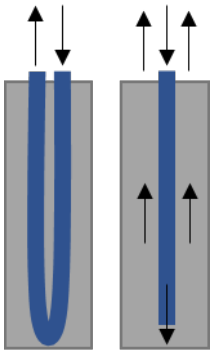

Figure 1-1. Borehole heat exchanger configurations: U-tube (left) and coaxial tube (right).

Although BHEs with coaxial pipe configuration show significantly better thermal performance than the more common U-tube BHEs (Acuña 2013), either single or double closed-loop U-tube BHEs have been used in most existing HT-BTES implementations (Sibbitt et al. 2012; Tordrup, Poulsen, and Bjørn 2017; Nußbicker et al. 2003; Mangold and Deschaintre 2015; Grycz, Hemza, and Rozehnal 2014). Coaxial type BHE installations have, however, been employed in a few HT-BTES applications in Sweden. A novel closed-loop tube-in-tube coaxial BHE using full-length steel casing as outer tube is currently being developed for the Filborna project in Helsingborg (Alkiswani and Regander 2019).

Low-permeability crystalline rock in combination with shallow depth to groundwater constitute suitable hydrogeological conditions for open-loop coaxial BHE installations, which have been implemented in the HT-BTES plants in Luleå and Emmaboda (Nordell 1994; Nordell et al. 2016). In open-loop BHE systems the

heat carrier fluid is directed down a single central pipe and flows through the annulus between the pipe and the borehole wall. Besides enhanced heat transfer capabilities, this solution is desirable since omission of the outer pipe allows for less material usage and smaller borehole diameters. However, given that a large-scale BTES may consist of hundreds or even thousands of boreholes, the use of submersible pumps or inefficient jet pumps is far from optimal to accomplish the circulation of the heat carrier fluid in the open-loop BHE network. In the Emmaboda case, this issue has been circumvented by operating the system under vacuum conditions using a circulation pump located at ground level (Nordell et al. 2016). Besides that such a solution is limited to sites where the groundwater table is sufficiently high for vacuum suction, there is an imminent risk of gas exsolution and cavitation or bulk boiling of the fluid when operating at high temperatures and low pressures. Thus, as the maximum operating temperature must be kept below the boiling temperature at a certain point, operating at too low pressures may be detrimental from an exergetic point of view.

Ideally, the tightness of the rock mass would be sufficiently high to permit for operation under positive head conditions without any substantial loss of circulation fluid. Because of their low degree of primary porosities and poor connectivity between voids, igneous and metamorphic rock matrices are apparently impermeable to water, i.e. they will transmit no or very small amounts of water under moderate pressures. Instead, fluid flow in hard rock takes predominantly place in preferential pathways created by interconnected joints and fractures.

If these pathways are sealed by means of introducing a sealing material into the fractures, an essentially impervious rock mass could potentially be achieved. This procedure, known as permeation grouting, is common in underground construction in order to reduce the inflow of water to the rock excavation and to mitigate subsequent environmental impacts due to groundwater drawdown. This is accomplished by drilling of a grouting fan around the excavation and injecting pressurized grout material into the fractures that intersect with the grouting fan boreholes.

A similar approach could possibly be adopted for implementing open-hole, single-pipe coaxial BHEs. The grout seal would in this case serve the purpose of preventing loss of water when the borehole is subjected to higher pressures than the ambient groundwater pressure, see Figure 1-2.

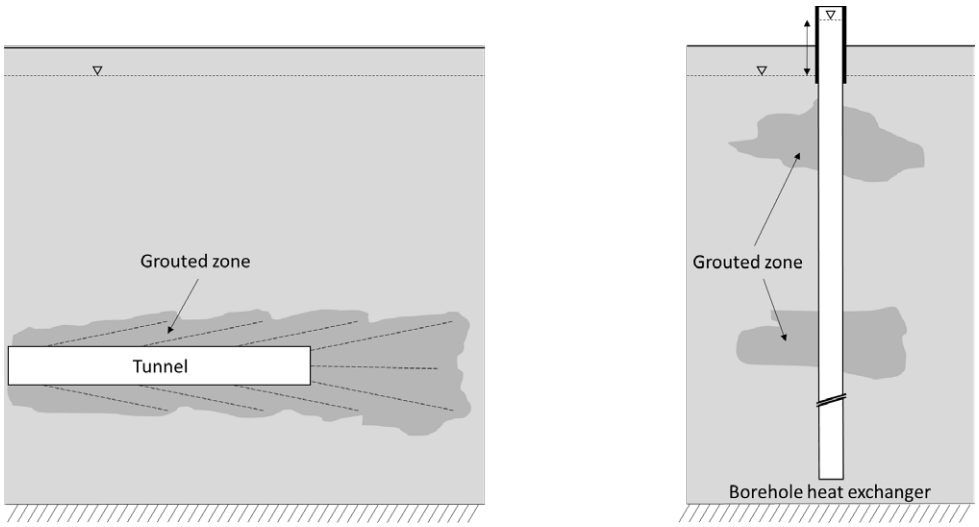

Figure 1-2. Reduction of water inflow into a tunnel (left) and reduction of water outflow from a borehole intented for high temperature thermal energy storage applications (right).

An ideally impermeable, single-pipe coaxial BHE would take advantage of both open- and closed-loop BHE designs and allow for efficient heat exchange with the rock at higher operating pressures and temperatures than what is possible using existing open-hole BHE designs.

1.2 SCOPE AND METHODOLOGY OF STUDY

This pilot study has focused on the application of permeation grouting techniques as a means of preventing or reducing fluid losses in open-hole pressurized boreholes.

The study aimed to investigate, develop and test possible approaches to achieve maximum sealing performance in grouted sections of boreholes.

The project comprised the following three stages:

Stage 1: Development of an approach for grouting and evacuation of fresh grout from the borehole section in order to enable re-access to the borehole and evaluating sealing effects achieved after grouting. A literature review was carried out focusing on fractured rock mass characteristics, properties of grout materials and grouting techniques, and their importance on the grouting result. A grouting design methodology based on criteria for avoiding mechanical breakdown of fresh grout was developed, with the aim of permitting grout evacuation and immediate post-grouting hydraulic testing without impairing the effect of sealing.

Stage 2: in-situ pre-investigations were carried out in two vertical, adjacent boreholes located at a candidate site for a large-scale HT-BTES plant. The objective was to investigate the hydrogeological conditions of the undisturbed rock at the site prior to grouting. A second objective was to collect data used for planning of the grouting field experiments in Stage 3 and establishing a grouting base design.

Stage 3: Demonstration of the approach developed in Stage 1 under practical conditions. The work comprised field experiments involving hydraulic testing and grouting in the boreholes that were investigated in Stage 2. Pre- and post-grouting

hydraulic tests were carried out with the objective of evaluating sealing efficiencies achieved in grouted borehole sections as a result of the grouting efforts. The results show that

The present report presents the details of the work carried out in these stages. Although the experimental work only involved small-scale field experiments in thermally undisturbed rock, the prospects for implementing the solution in large-scale, long-term operation of HT-BTES systems are also briefly discussed.

2 Literature review

Fracture sealing by permeation grouting requires good understanding and knowledge of the rock mass, the groundwater, the grout material characteristics and the grouting performance, i.e. the choice of pressure, flow and time during grouting. When implementing densely populated borehole fields for grouting and heat exchange applications, drilling becomes another factor to consider. In this section, a review of the abovementioned parameters, and how their interaction influences the result of the grouting, is provided.

2.1 HARD ROCK HYDROGEOLOGY

In igneous and metamorphic rock, the ability of the rock mass to transmit fluids is predominantly dependent on the appearance of the fracture network within the rock mass. The intergranular matrix has little porosity and may in practice be impermeable. The fracture characteristics and degree of fracturing of a rock mass depend on the site-specific geological history (e.g. rock formation process, stress history etc.) and the rock properties (e.g. chemical composition, mechanical properties such as brittleness/ductility etc.) (Gustafson 2009). The importance of lithology for the hydrogeological characteristics of fractured hard rock has been review by (Wahlgren et al. 2015; Olofsson et al. 2001; Banks, Rohr-Torp, and Skarphagen 1994), among others. It has been demonstrated that some hard rock lithologies statistically show higher median water yield capacity than others (Banks, Rohr-Torp, and Skarphagen 1994). For example, rock types with high content of silica, i.e. acidic rocks such as granite, tend to be more brittle and fracture-prone than basic rock types such as gabbro and amphibolite (Olofsson et al. 2001). It is however important to note that median variations in water yield (or permeability) in boreholes in different lithologies are smaller than differences in boreholes within a specific lithology (Banks, Rohr-Torp, and Skarphagen 1994).

Various measures are used to describe the hydrogeological properties of a rock mass. The intrinsic permeability (m^2) is a property of the rock mass itself, while the closely related terms hydraulic conductivity (m/s) and transmissivity (m^2/s) also incorporate the density and viscosity of the fluid. These measures are also properties applicable to single fractures; depending on the fracture intensity, fracture permeabilities and degree of connectivity, the individual fractures form a network that is more or less permeable to for example water. It should be noted that non-percolating fractures, i.e. isolated fractures or fracture clusters within a rock mass, do not contribute to fluid flow.

Fluid flow in a permeable medium is governed by hydraulic head differences throughout the ground, i.e. hydraulic gradients. According to (Darcy 1856), laminar flow (Q) through a cross-sectional area (A) in a porous medium with hydraulic conductivity K can be expressed as

$$Q = -KA\frac{dh}{dx} \qquad (2\text{-}1)$$

where dh/dx is the hydraulic gradient. The transmissivity T of an aquifer with thickness b_a or a borehole section of length L is linearly proportional to the hydraulic conductivity according to the relationship

$$T = Kb_a = KL \quad (2\text{-}2)$$

A detailed review of fractured rock hydrogeology in the area of underground construction is provided in (Gustafson 2009). In grouting applications, the spatial scale of the problem that needs to be considered ranges from individual fractures to, say, the size of the borehole or the tunnel that is constructed. Predicting and measuring hydraulic properties of fractured rock is often a difficult task due to fracture characteristics being highly spatially irregular on different scales. On the scale of a single fracture plane, the aperture may be non-uniform, partly occupied by infilling materials or at some spots closed (Byegård et al. 2017). This creates preferential flow paths within the fracture plane following the direction of the head gradient. In a study by (Abelin et al. 1985), it was found that the flow was distributed along distinct channels making up only 5-20% of the fracture plane. The transmissivity of a fracture is however commonly estimated by assuming laminar flow between two parallel plates with spacing b_h (Snow 1965):

$$T = \frac{\rho_w g {b_h}^3}{12\mu_w} \quad (2\text{-}3)$$

In Equation (2-3), ρ_w and μ_w are the density and viscosity of the fluid and g is the acceleration due to gravity. This equation is referred to as the cubic law, as the fracture transmissivity is proportional to the cube of the so-called hydraulic aperture, b_h.

Variability in for example fracture intensities, sizes and orientations (strike and dip) appears also on larger scales, which causes the properties of the rock to be highly heterogeneous and anisotropic (Dietrich et al. 2005). Since fracture characteristics are difficult, if not impossible, to determine deterministically, it is common to describe the fracture properties by means of statistical distributions estimated from field observations.

A statistical approach for describing fracture transmissivities and hydraulic apertures based on borehole field data was originally suggested by (Fransson 2002) and (Gustafson et al. 2004). The method is well presented in the literature (Fransson 2008; Gustafson 2009; Thörn et al. 2015) and has been applied in several grouting projects (Funehag and Gustafson 2005; Butron, Gustafson, and Funehag 2008; Funehag and Emmelin 2011). Two sets of data are required as input to the statistical analysis, the first one being the lineal fracture intensities expressing the number of fractures per unit length, the second one being the transmissivity estimates of sections along a borehole. The lineal fracture intensity along the borehole, commonly denoted by P_{10} (Dershowitz and Herda 1992), is obtained from core mapping or from optical/acoustic borehole logging tools. Interval transmissivity estimates can be evaluated from constant head double-packer tests, for example by using the well-known Moye formula with the assumption of steady state radial flow in a homogeneous continuum (Moye 1967),

$$T_{Moye} = \frac{Q\rho_w g}{2\pi dp}\left[1 + \ln\left(\frac{L}{2r_b}\right)\right] \quad (2\text{-}4)$$

where Q is the fluid flow, dp is the injection differential pressure, L is the interval length and r_b is the borehole radius.

Following the approach described by (Fransson 2002), the interval transmissivity data are used to estimate the number of intervals (I_T) out of the total number of intervals (I) having a transmissivity smaller than T_i. Assuming that all fractures are independent (statistically as well as hydraulically), and that the largest fracture within a tested interval accounts for almost all of the fluid loss, the multiplication principle can be used to set up the approximate equality,

$$I_T \approx \sum_{i=1}^{I} p(T < T_i)^{N_i} \quad (2\text{-}5)$$

where N_i is the number of conductive fractures in the ith interval. If the interval transmissivity estimates are sortered in ascending order, Equation (2-5) can by iteration be solved for $p(T < T_i)$ for each of the I estimates. The approximate solutions can be plotted in a cumulative distribution chart, where they represent the probability of a fracture having lower transmissivity than the largest fracture in each interval. (Gustafson and Fransson 2005) found that evaluated fracture transmissivities could be well-fitted by a Pareto or power-law distribution, which supports the observation that in many cases a large portion of the fractures have relatively low transmissivity and a few large fractures make up the main contribution to the total transmissivity. If plotted in a log-log cumulative probability chart, the Pareto distribution is shown as a straight line with a slope of $-k$, according to

$$\log[1 - p(T)] = \log\left[\frac{T_{max}^k}{N+1}\right] - k\log[T] \quad (2\text{-}6)$$

where T_{max} is the maximum fracture transmissivity and N is the total number of fractures. The distribution parameters $T_{max}^k/(N+1)$ and k can be determined by linear regression of the data set obtained from solving Equation (2-5). Expressing a distribution of hydraulic apertures is then straigthforward using the relationship between fracture transmissivity and aperture shown in Equation (2-3). If r denotes the rank in an ordered sample of N fractures, the hydraulic aperture of the fracture can be given by

$$b_r = \frac{b_{max}}{r^{1/3k}} \quad (2\text{-}7)$$

where b_{max} corresponds to the hydraulic aperture of the largest fracture (Gustafson and Fransson 2005).

Knowledge of fracture hydraulic apertures is of central importance in grouting design, as will be shown in Section 2.2. It should however be noted that the method described above is based on simplifying assumptions, one being that fractures are independent two-dimensional features with cylindrical flow. To gain further understanding of fluid flow and grouting processes in fractured rock, it is important to pay attention to fracture geometries, boundary effects and spatial flow dimensions, i.e. whether the flow can be described as linear (1D), cylindrical

(2D) or spherical (3D). For example, grouting of fractures characterized by 1D channeled flow is generally considered more difficult than in the case of 2D flow, since it is less probable to intersect the part of the fracture that is connected to the conduit network (Fransson 2008). The hydraulic geometry of the rock can be characterized by means of evaluating the transient behaviour of the flow/pressure response during single or multiple well testing. Although not detailed further here, several thorough studies and reviews on the topic can be found in the literature (Doe and Geier 1990; Dershowitz 1984; Karasaki 1986; Carlsson and Gustafson 1984).

2.2 PERMEATION GROUTING IN HARD ROCK

2.2.1 Properties of grout materials

Grout materials can generally be divided into two main categories; cementitious and non-cementitious grouts, respectively. Cement suspension grouts consist of a mixture of cement and water with a certain water to cement ratio (WCR). Sometimes additives, e.g. superplasticizers or accelerators, are added to the grout mix to modify the rheological or mechanical behaviour of the cement-based grout.

Non-cementitious grouts are used less frequently than cementitious dittos; due to their environmental impact most chemical grouts have seen very limited use in Sweden, the exceptions being colloidal silica, or silica sol, and polyurethane (Axelsson 2009). Recently, stricter demands for reducing the amount of water ingress into underground excavations have raised attention on these materials due to their high penetrability and capability of sealing very narrow fractures. The use of polyurethane and colloidal silica in grouting applications has been investigated by (Andersson 1998) and (Funehag 2007), respectively. Only cement-based grouts and silica sol were used for the field experiments carried out in this study. Thus, polyurethane grouts are not covered further in this report.

Both cement-based and silica sol grouts are suspensions consisting of solid particles dispersed in a liquid phase. The strength development of cement-based grout occurs during a setting process after mixing of cement and water. Silica sol form a solid gel in a sol-gel process when mixed with a saline solution. While most cement-based grouts consist of cement grains having maximum grain sizes in the range of 16-30 μm (Axelsson 2009), silica particles are significantly more fine grained with diameters between 5-100 nm (Funehag 2007). Grain size and grain size distribution are some of the factors affecting the penetrability (the ability to penetrate fracture apertures of certain sizes) and the filtration tendency (the property that governs the tendency of grains clogging and preventing further penetration) of the grout. These properties have been subjects of extensive research in recent years (Eklund 2005; Draganovic 2009; Martinet 1998). (Eklund 2005) showed that too small cement grain sizes may deteriorate the filtration tendency due to grains forming agglomerates by flocculation. One conclusion of the study was that the aperture of the fracture should be between than 2-16 times the size of the d_{95} of the cement in order to avoid filtration. Indeed, fracture apertures smaller than approximately 100 μm are in general not considered to be penetrable by cement grouts (Gustafson 2009). Silica sol shows however significantly higher

penetrability due to its small particle sizes. In field experiments it has been used for sealing of fractures at least as narrow as 10 μm (Funehag 2007; Funehag and Gustafson 2008a).

In addition to the penetrability and filtration tendency, the fluid flow and spread within a fracture is affected by the rheological properties of the grout. Initially before any hardening process has started, the rheological behaviour of cement-based grouts vs. silica sol is fundamentally different. Silica sol shows Newtonian behaviour, while cement-based grouts are yield stress fluids, i.e. the fluid is only able to flow when exposed to a stress exceeding its yield stress. Usually the Bingham model is applied to describe the flow behaviour of cement-based grouts:

$$\tau = \tau_0 + \mu_B \dot{\gamma} \qquad (2\text{-}8)$$

where τ_0 is the yield stress, μ_B is the dynamic viscosity and $\dot{\gamma}$ is the shear rate. This is a simplified model, in reality cement-based grouts show thixotropic behaviour meaning that their true rheological properties are variable depending on shear history (Håkansson 1993). Newtonian fluids also show a linear relationship between shear stress and shear rate, with zero yield stress and constant viscosity:

$$\tau = \mu_N \dot{\gamma} \qquad (2\text{-}9)$$

As will be shown in Section 2.2.2, the penetration of a Bingham fluid is only dependent on its yield stress and viscosity. The gelling process of silica sol is however related to a time dependent growth in viscosity occuring relatively soon after mixing with saline solution. It is characterized by the gel induction time, t_G, which is defined as the time at which the initial viscosity, μ_0, has grown double. Another important property is the gel time, that is the time from mixing until the fluid contained in a beaker does not flow when tilting the beaker 90°. The gel induction time and gel time depend on the mixing ratio of silica sol and saline solution. A general rule says that the gel time is around three times as large as the gel induction time (Funehag 2012).

Regarding the risk of erosion of the grout, as will be dealt with in Section 2.2.3, the final strength after the hardening process is not of great importance (Axelsson 2009). Instead, it is more likely that erosion will occur during or early after the grout is injected. Thus, the initial strength and early strength development of the grout is crucial. Investigations of strength development and methods to measure rheological and mechanical properties in field or laboratory are presented in (Håkansson 1993; Axelsson and Gustafson 2006; Butrón, Axelsson, and Gustafson 2009; Ranta-Korpi, Karttunen, and Sievänen 2008; Rahman and Håkansson 2011) among others. Rheological properties and strength characteristics of cement-based grouts can be adjusted by varying the WCR or by adding additives, for example when a higher initial yield stress or shorter setting time is desired. As mentioned above, the strength development of silica sol grouts is governed by the amount of salt added to the mixture, but it should also be considered that the gel time is strongly temperature dependent, with decreasing gel time with increasing temperature (Funehag 2012; Butrón, Axelsson, and Gustafson 2009).

2.2.2 Grout penetration

Recent advances in grouting simulations and analysis of Bingham and gelling fluid flow have made it possible to predict the spread and penetration of the grout. The penetration length is the distance from the grout source to the front of the grout plume. The penetration obtained is a result of the combination of rock and groundwater characteristics, the rheology of the grout and the grouting time and pressure. Hence it is an important parameter in grouting design.

Cement-based grouts

(Gustafson and Stille 2005) presented an analytical method to predict the transient spread of a Bingham fluid in smooth 1D conduits and 2D parallel plane fractures. The maximum attainable (theoretically) penetration length can be calculated according to

$$I_{max} = \frac{\Delta p \cdot b_h}{2\tau_0} \quad (2\text{-}10)$$

where Δp is the difference between the grouting pressure and the groundwater pressure, b_h is the hydraulic aperture and τ_0 is the yield strength of the grout. The characteristic time t_0 and the dimensionless time t_D are defined as

$$t_0 = \frac{6\mu_B \Delta p}{{\tau_0}^2},\ t_D = \frac{t}{t_0} \quad (2\text{-}11)$$

where μ_B is the Bingham viscosity and t is the actual grouting time. The relative penetration I_D relates the maximum penetration length to the actual penetration length,

$$I_D = \frac{I}{I_{max}} \quad (2\text{-}12)$$

The derivation of the relative penetration results in an implicit equation. An approximate solution for the cases of 1D and 2D features is given by (Gustafson and Stille 2005):

$$I_D = \sqrt{\theta^2 + 4\theta} - \theta,\ \theta_{1D} = \frac{t_D}{2(0.6+t_D)},\ \theta_{2D} = \frac{t_D}{2(3+t_D)} \quad (2\text{-}13)$$

Silica sol grouts

For a gelling fluid as silica sol, the material undergoes rapid change in rheology characteristics as compared to cement-based grouts. Hence the gelling process will affect the penetration length (Funehag 2007). (Funehag and Gustafson 2008b) developed a calculation method for predicting the penetration length of silica sol accounting for the viscosity development over time. The viscosity change as a function of time can be expressed by

$$\mu_g = \mu_0 \left[1 + e^{\alpha\left(\frac{t}{t_G}-1\right)}\right] \quad (2\text{-}14)$$

where μ_0 is the initial viscosity, t is the time and t_G is the gel induction time. The dimensionless parameter α must be determined experimentally. By introducing the scaling factor

$$I_G = b_h \sqrt{\frac{\Delta p t_G}{6\mu_0}} \qquad (2\text{-}15)$$

the actual penetration can be expressed $I = I_G \cdot I_D$, where I_D is the dimensionless penetration. By assuming 1D channel flow and introducing the dimensionless time t_D according to $t = t_G \cdot t_D$, the dimensionless penetration can be calculated as follows:

$$I_{D,1D} = \sqrt{t_D - \frac{1}{\alpha}\ln\left(\frac{e^{\alpha} + e^{\alpha t_D}}{e^{\alpha} + 1}\right)} \qquad (2\text{-}16)$$

The asymptote of $I_{D,1D}$ approaches 1 for very high t_D, meaning that I_G is the maximum penetration length of gelling silica sol in case of 1D channel flow (Funehag and Gustafson 2008b). Likewise, in the case of 2D radial flow, $I_{D,2D}$ can be calculated by introducing the dimensionless borehole radius r_D according to $r_b = r_D \cdot I_G$, and solving the implicit equation

$$t_D - \frac{1}{\alpha}\ln\left(\frac{e^{\alpha} + e^{\alpha t_D}}{e^{\alpha} + 1}\right) = I_{D,2D}^2\left[\ln\left(\frac{I_{D,2D}}{r_D}\right) + \frac{1}{2}\right] - \frac{r_D^2}{2} \qquad (2\text{-}17)$$

An iterative algorithm for solving Equation (2-17) with respect to $I_{D,2D}$ is given in (Funehag and Gustafson 2008b). It can be shown that a theoretical limit of 2D radial penetration of gelling silica sol is $I_{2D} \approx 0.45 I_G$.

Other theoretical studies on the topic of grout penetration are presented by (Gustafson, Claesson, and Fransson 2013; Funehag and Claesson 2017; El Tani and Stille 2017) among others. Experimental tests in laboratory have been carried out by (Funehag and Thörn 2018; Mohammed, Pusch, and Knutsson 2015), and several field experiments following grouting designs based on the theory of penetration length have been carried out with satisfactory results (Funehag and Fransson 2006; Funehag and Gustafson 2008a; Kobayashi and Stille 2007).

2.2.3 Mechanical breakdown of fresh grout

When constructing underground excavations open to the atmosphere, a hydraulic gradient field will be induced in the region close to the excavation and surrounding groundwater will tend to flow towards the excavated low-pressure zone. The hydraulic gradient implies that the groundwater exerts a force on the grout. If the shear stresses from water flow exceed the strength of the grout, a breakdown process known as erosion will eventually occur. In the application dealt with in this study, hydraulic gradients will intentionally be induced due to borehole pressurization when performing post-grouting hydraulic tests and during continuous operation of the HT-BTES. That is, the risk of erosion must be considered in the grouting design process.

Mechanical breakdown processes in permeation grouting applications have been studied by (Axelsson 2009; Funehag 2017). (Axelsson 2009) identified three main processes affecting mechanical breakdown of the grout:

- Erosion, which occurs due to shear stresses from flowing water exceeding the shear strength of the grout.

- Fingering, which is dependent on viscosity differences and occurs if the pressure gradient of the grout is lower than the gradient of the water. Instead of grout replacing the water as is intended, fingering results in water penetrating the upstream intruding grout plume.
- Back-flow, which occurs due to water forces exceeding the adhesive forces that bond the grout to the surfaces of the fracture.

According to (Funehag 2017), mechanical breakdown because of erosion is prevented by ensuring that the shear strength of the grout is larger than the driving shear stress from the water motion at the end of the grouting process. Back-flow can be prevented by achieving a penetration length sufficient to balance the fracture-grout interface friction forces with the water pressure. Fingering is prevented by employing a resolute grouting pressure and by ensuring that the viscosity of the grout is higher than that of the water. Additionally, turbulence considerably increases the risk of erosion to occur (Fransson and Gustafson 2006). The transition from laminar to turbulent fracture flow occurs at Reynold number ≈ 10 (Zimmerman 2005).

Assuming laminar plane Poiseuille flow in a fracture with hydraulic aperture b_h, the shear stress due to the water pressure p_w acting over the penetration length I can be written (Smits 2000)

$$\tau_w = \frac{b_h}{2}\left(-\frac{p_w}{I}\right) = \frac{b_h \rho_w g}{2}\left(-\frac{dh}{dx}\right) \qquad (2\text{-}18)$$

where dh/dx is the hydraulic head gradient. A criterion for avoiding back-flow or erosion of a fluid with yield stress τ_g is (Fransson and Gustafson 2007)

$$\tau_g \geq \tau_w = \frac{b_h \rho_w g}{2}\left(-\frac{dh}{dx}\right) \qquad (2\text{-}19)$$

(Axelsson 2009) summarizes the parameters affecting mechanical breakdown of grouts, which are shown in Table 2-1.

Table 2-1. Summary of parameters affecting the mechanical breakdown of grouts (Axelsson 2009).

Rock mass	Grout	Grouting performance
Fracture aperture, groundwater pressure, hydraulic gradient, Reynolds number	Grout penetrability, grout rheology, initial strength of the grout	Grouting pressure and flow, grouting time

2.3 DRILLING TECHNIQUES FOR SHALLOW GEOTHERMAL ENERGY SYSTEMS

In the construction of BTES plants, large arrays of boreholes are drilled in a dense and compact pattern typically with a spacing of 3-7 m (Skarphagen et al. 2019).

In Scandinavia, down-the-hole (DTH) hammer drills are by far the most widely used for BTES installations in hard rock. The vast majority of these are drilled with air-powered DTH equipment, but in recent years also water-driven DTH drilling has become more widely used. In DTH drilling, a pressurized fluid is directed

through the drill string to the downhole hammer, where part of the potential energy is converted into kinetic energy and transferred to the drill bit by piston impacts. The percussive motion is combined with a rotary motion of the drill bit, thus giving new contact points between the drill bit buttons and the rock as the piston cycle is repeated.

Both DTH drilling methods essentially share the same working principle, the main difference being the driving pressures and the fluid (air/water) used for energy transferring and hole flushing. When drilling with a pneumatic system in water-rich environment, the maximum depth that theoretically can be reached is limited by the height of the water column in the borehole, the pressure of the air and thus the compressor capacity (Nordell, Fjällström, and Öderyd 1998). For water-driven systems the hammer can work at virtually any depth. Since air is a compressible fluid, the air will expand and reach very high velocity as it exits the drill bit and rises up the annulus between the drill string and the borehole wall. Using an incompressible fluid, with higher density and viscosity than air, allows for significantly lower flushing velocity yet sufficiently high to transport drill cuttings to the top of the borehole. At such moderate uphole velocities, erosion of the drill pipes is reduced which permits the use of close-fitting stabilizers to achieve higher borehole accuracy (Tuomas 2004; D. D. A. Bruce, Lyon, and Swartling, n.d.).

The damaging or disturbing effect of drilling operations may cause a near-borehole alteration in permeability due to mechanical alteration or invasion of drilling fluids, in the literature commonly denoted as “skin effect” (Kroehn and Lanyon 2018). This skin effect can be both positive and negative. Comparative studies concerning the influence on the skin effect of different DTH methods have not been found. In permeation grouting applications, however, the use of air-powered DTH techniques has been prohibited since air-flushing promotes the risk of rock debris entering and blocking the fractures, thus possibly preventing grout penetration. Flushing the borehole using water is therefore recommended (Warner 2004; D. Bruce 2012).

3 Pre-investigations and hydrogeological characterization

Below are presented descriptions of the investigation site and the activities performed to collect borehole data for rock mass characterization. The investigation site, located at Distorp, Linköping, has been identified as a candidate site for a large-scale HT-BTES plant intended for integration with the Linköping district heating network (Lindståhl 2018). Extensive multidisciplinary field investigations have been conducted for characterizing the thermal, geological and hydrogeological conditions at the site. The main focus in this section is on the hydraulic tests and geophysical wire-line surveys performed to provide input data for establishing a preliminary grouting design (see Section 4) prior to the grouting field experiments (see Section 5).

3.1 SITE DESCRIPTION AND BOREHOLE DIRECTIONAL SURVEYS

The investigation site is situated in the transitional zone between the Småland and Bergslagen lithotectonic units, which are bounded by the NW-SE striking Loftahammar-Linköping Deformation Zone (LLDZ), see Figure 3-1. The bedrock in the area is dominated by granite, gneissic granitoids and metabasite. The quaternary deposits covering the bedrock consists of a 5-10 m thick layer of glacial sandy-silty till and postglacial clay.

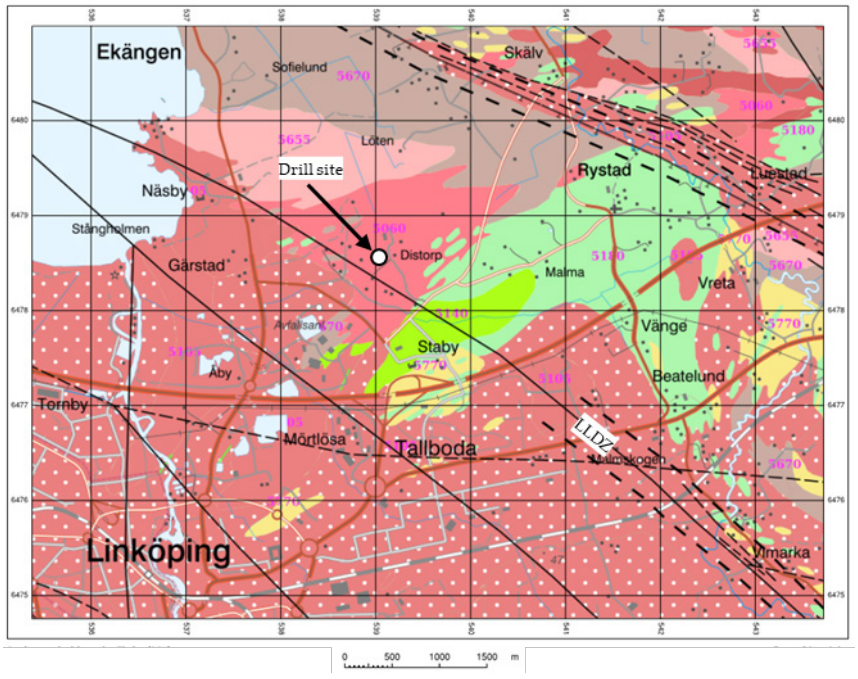

Figure 3-1. Location map showing the investigation site and deformation zone traces in the area. The Loftahammar-Linköping Deformation Zone (LLDZ) is a large-scale, NW-SE striking, subvertically dipping shear zone that forms the boundary between the Småland and Bergslagen lithotectonic units. From (SGU Sveriges Geologiska Undersökning n.d.).

At the investigation site, two medium deep investigation boreholes (DH-BH1L, DH-BH2V) and three shallow monitoring boreholes (DH-OH1, DH-OH2, DH-

OH3) have been established. The borehole arrangement is shown in Figure 3-2. Borehole DH-BH1L was drilled in November 2017 using a pneumatic down-the-hole (DTH) percussion drill. In September 2018, DH-BH2V and the peripheral monitoring boreholes were drilled by means of a water-powered DTH system adjacent to the existing borehole.

Drill cuttings recovered during drilling of DH-BH1L show that the lithology is dominated by fine-grained red and grey granites, with elements of medium-grained granodiorite. The uppermost rock layer (c. 30 m thick) consists of sedimentary rock, probably sandstone. The groundwater table is located at a depth of between 2 and 3 m below the ground surface.

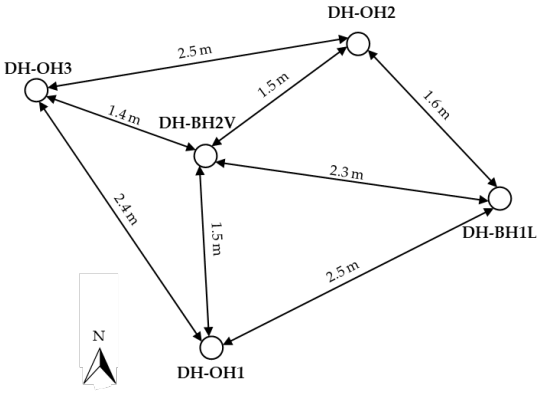

Figure 3-2. Arrangement of boreholes at the investigation site. The entry points of investigation boreholes DH-BH1L and DH-BH2V are located with a spacing of 2.3 m relative to each other.

Deviation measurements were conducted in DH-BH1L and DH-BH2V to achieve information on dip and azimuth angles along the boreholes. Horizontal and vertical projections of the borehole trajectories are shown in Figure 3-3.

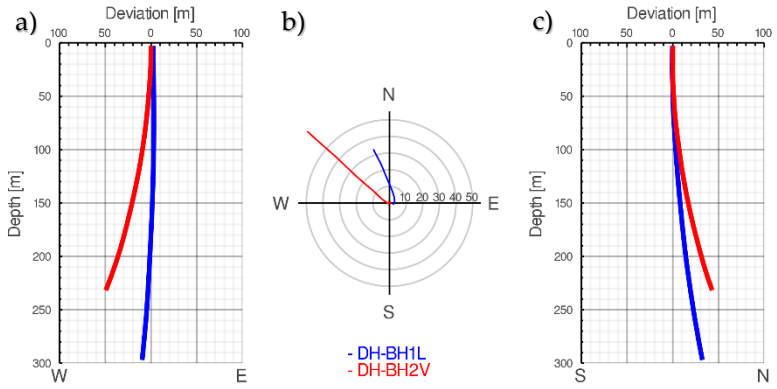

Figure 3-3. Borehole projections onto a) vertical E-W plane b) horizontal plane c) vertical N-S plane.

As shown in Figure 3-3 a), the boreholes tend to deviate to the NW and NNW. The conceived straight line intersecting the collaring point and the end point of DH-BH1L has a bearing of -20° compared to the north and an inclination of about 7° from the desired vertical course. Although water-powered DTH systems generally allows for more accurate drilling compared to conventional pneumatic systems (Nordell, Fjällström, and Öderyd 1998), the borehole departure of DH-BH2V is significantly higher with inclination and bearing angles of 16° and -49°, respectively. A summary of borehole geometric details is presented in Table 3-1.

Table 3-1. Summary of borehole details.

Hole ID	Type	Borehole length (m)	Drill bit diameter (mm)	Target inclination	Inclination	Bearing	Casing (m)
DH-BH1L	Investigation/grouting	300	115	0°	7°	-20°	9
DH-BH2V	Investigation/grouting	244	89	0°	16°	-49°	8.5
DH-OH1	Monitoring	30	89	0°	-	-	
DH-OH2	Monitoring	30	89	0°	-	-	
DH-OH3	Monitoring	30	89	0°	-	-	

3.2 WIRE-LINE GEOPHYSICAL LOGGING

In October 2018, geophysical logging of boreholes DH-BH1L and DH-BH2V was conducted by Geological Survey of Sweden (SGU) as part of the GeoERA MUSE-project (GeoERA 2019). Among the logs that were carried out are caliper, natural gamma, spontaneous potential, normal resistivity and single point resistance (SPR) logs. In addition, acoustic imaging was conducted using an acoustic televiewer (ATV) probe to provide continuous, 360° panoramic views of the borehole walls. The combination of the logs provides a means for locating major water-bearing fractures, estimating fracture intensities along the boreholes and detecting possible hydraulical connections between the boreholes.

ATV imaging systems use an ultrasonic pulse-echo reflection technique to record the transit time and amplitude of the acoustic signal returning from the borehole wall. The transit time and amplitude data reveal borehole enlargements and can be used for generating 360° caliper (i.e. diameter) logs. Lithological changes, foliations or sealed fractures may also be detected due to contrasts in acoustic impedance of the borehole wall, making it sometimes unclear whether detected anomalies are actually open, transmissive fractures (Williams and Johnson 2004). However, planar features appear on unwrapped ATV images as more or less sinusoidal traces, depending on the dip of the feature relative the borehole axis (Figure 3-4). It is thus possible to determine the location and other geometric characteristics of a detected fracture if the borehole trace is known. In this study only the locations of fractures relative to the borehole length were considered.

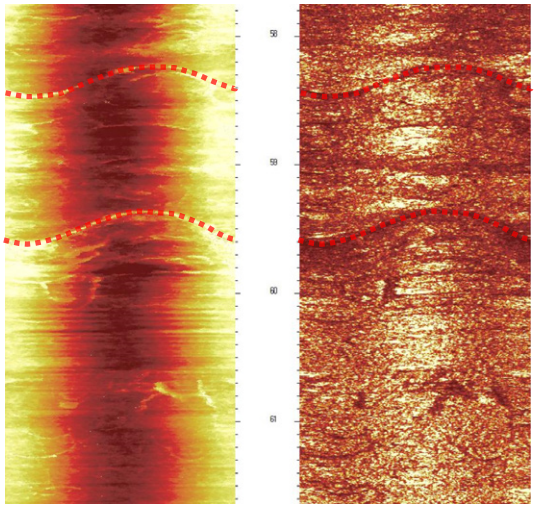

Figure 3-4. Fracture traces appearing on transit time (left) and amplitude (right) image logs.

ATV images were manually analyzed and interpreted in order to estimate the lineal fracture intensities, P_{10}, along boreholes DH-BH1L and DH-BH2V down to a depth of 65 m. Since no core was acquired from any of the boreholes it is not possible to corroborate that a detected fracture is open and transmissive, though the largest conductive fractures can be clearly recognized on the combined geophysical logs, as can be seen in Section 3.5 . It was however assumed that all fractures detected on the ATV logs contribute to transmissivity, and therefore accounted for when estimating lineal fracture intensities.

The SPR (measured in Ω) and normal resistivity (measured in Ω·m) logs were used for qualitative detection of anomalies indicating water-bearing fractures and fracture zones. The SPR logs are conducted by measuring the current and voltage of a power source and calculating the resistance between a surface current electrode and an inhole current electrode using Ohm's law. The normal resistivity log is carried out by also lowering a potential electrode at a certain distance from the inhole current electrode and measuring the potential drop between the inhole electrodes. The radius of investigation and the vertical resolution depend on the inhole electrode arrangement. Both short normal (spacing 0.4 m) and long normal (spacing 1.6 m) resistivity measurements were conducted. SPR and short normal resistivity measurements are better suited for detection of minor anomalies but are more dependent on the resistivity of the borehole fluid than long normal resistivity measurements, which have poor vertical resolution but provide better information on the true resistivity of the formation due to greater investigation depths (Löfgren and Neretnieks 2003). Measurements of natural gamma radiation along the borehole may sometimes be used in combination with the electrical logs for better interpretion of detected anomalies. Although the primary use of natural gamma measurements is for lithological investigations, anomalies detected in the gamma ray log may indicate radioisotope concentrations present in infilling materials of fractures (Paillet 1994). The combined electrical and natural gamma logs conducted in boreholes DH-BH1L and DH-BH2V are presented in Section 3.5.

3.3 HYDRAULIC TESTING

Hydraulic tests were conducted in boreholes DH-BH1L and DH-BH2V in February 2019. The tests were performed with two primary objectives: 1) to investigate the hydrogeological conditions of the undisturbed rock. i.e. prior to grouting, in order to determine existing conditions as a base for future comparisons of borehole tightness, 2) to collect data used as input to the grouting base design.

The hydraulic testing campaign was carried out with the aim of determine the transmissivity and hydraulic conductivity by water loss measurements (WLM) in multiple intervals of varying sizes along the full length of the boreholes. The test procedure involves isolating a borehole section with an inflatable single or double packer and injecting water into the fracture system. During the injection phase the pressure is kept constant while the flow rate decreases and approaches a stable value.

The inhole equipment consists of a double packer system mounted on a pipe-string that is lowered down the hole using a hoisting rig. The packer-to-packer distance can be adjusted by coupling pipe sections of 2 or 3 m length together. The test section pressure is measured using a submersible pressure sensor that is used for both pressure-flow regulation and test evaluation. The pressure is controlled using a device consisting of a regulation and data acquisation system with integrated pumps and two flow meters for low-flow and high-flow measurements, respectively.

Details of the flow measurements are shown in Table 3-2. The lower measurement limit for the hydraulic tests was set to 5 ml/min, although the measurement limit of the low-flow meter is lower. Due to limited pump capacity, the upper practical measurement limit was set to 60 l/min.

Table 3-2. Measurement limits and flow meter specifications.

Flow measurement data		Comment
Lower measurement limit	0.005 l/min	-
Upper measurement limit	60 l/min	Due to pump capacity limitations
Flow meter (low flow)	0.002-1.6 l/min	Accuracy:
		<0.0002 l/min (0.002-0.1 l/min)
		<0.5% (curr. value, > 0.1 l/min)
Flow meter (high flow)	1.0-100 l/min	Accuracy:
		< 0.5% (curr. value)

The test program involved measurements using double packer setups with section lengths of 5 m and 50 m. In addition, a few test were performed with single packers in the deepest sections of the boreholes . The use of 50 m setups was a compromise between desiring to characterize the entire borehole depths and avoiding a too extensive and time-consuming test procedure. The 5 m setups were

used for a more detailed characterization of some of the most interesting sections that had been identifed from the geophysical logs. These are mainly located in the uppermost parts of the boreholes (< ~60 m depth), though a few large fractures were found at greater depths.

For all the tests performed the injection pressure was maintained at a constant head of about 200 kPa above the groundwater pressure. Injection proceeded for about 15 minutes after stable pressure had been achieved. The transmissivity of all test sections were evaluated based on the quasi-steady flow measured in the end of the injection period, using Moye's formula assuming stationary flow conditions according to Equation (2-4). Results of the tests performed are summarized for DH-BH1L in Table 3-3 and for DH-BH2V in Table 3-4, and further discussed in Section 3.5. None of the measured flow rates were below the measurement limit of 5 ml/min.

Table 3-3. Results of water loss measurements in borehole DH-BH1L. All depths refer to measured depth from top of casing.

Section (m)	Section length (m)	Pressure head (kPa)	Flow rate (l/min)	T_{Moye} (m^2/s)	K_{Moye} (m/s)	Comment
11.2 - 61.2	50.0	201	28.4	2.6E-05	5.2E-07	Flow detected at top of casing
61.2-111.2	50.0	200	17.8	1.6E-05	3.3E-07	Flow detected at top of casing
111.2- 161.2	50.0	199	0.91	8.4E-07	1.7E-08	
161.2-211.2	50.0	200	1.16	1.1E-06	2.1E-08	
211.2 -261.2	50.0	200	14.9	1.4E-05	2.7E-07	
211.2-300.0	88.8	200	15.4	1.5E-05	1.7E-07	Single packer at 211.2 m
19.5-24.5	5.0	199	8.2	5.1E-06	1.0E-06	
24.5 -29.5	5.0	199	3.3	2.0E-06	4.1E-07	
38.0-43.0	5.0	200	13.9	8.6E-06	1.7E-06	
44.0-49.0	5.0	200	22.9	1.4E-05	2.8E-06	Flow detected at top of casing

Table 3-4. Results of water loss measurements in borehole DH-BH2V. All depths refer to measured depth from top of casing.

Section (m)	Section length (m)	Pressure head (kPa)	Flow rate (l/min)	T_{Moye} (m^2/s)	K_{Moye} (m/s)	Comment
14.0-64.0	50.0	200	11.0	1.0E-05	2.1E-07	
64.0-114.0	50.0	200	7.7	7.3E-06	1.5E-07	
115.0-165.0	50.0	200	3.4	3.2E-06	6.5E-08	
165.0-215.0	50.0	200	0.35	3.3E-07	6.6E-09	
165.0-244.0	79.0	200	0.50	5.1E-07	6.6E-09	Single packer at 165.0 m
8.0-244.0	236.0	199	36.5	4.2E-05	1.8E-07	Single packer at 8.0 m
20.0-25.0	5.0	199	2.81	1.8E-06	3.7E-07	
25.0-30.0	5.0	200	0.16	1.0E-07	2.1E-08	
40.5-45.5	5.0	200	1.14	7.5E-07	1.5E-07	
47.5-52.5	5.0	200	0.55	3.6E-07	7.3E-08	
83.0-88.0	5.0	200	6.5	4.2E-06	8.5E-07	

3.4 THERMAL TESTING

Thermal tests were performed in DH-BH1L and DH-BH2V, including Distributed Thermal Respons Tests (DTRT) and point-source heat tracing tests using immersion heaters with distributed fiber-optic temperature sensing. In DH-BH1L, one hydraulic, full-length DTRT was performed in a single U-tube heat exchanger that was temporarily installed in the borehole. In DH-BH2V, two open-hole DTRTs were conducted on different occasions. Since no piping was installed, the heat injection was accomplished by means of a heating cable inserted into the borehole at overlapping depth intervals.

In these tests, temperature profiles in the borehole are continuously recorded before, during and after heat injection. Possible groundwater movements can be detected by examining temperature anomalies in the thermal recovery phase of the tests.

3.5 SUMMARY OF BOREHOLE INVESTIGATIONS

Investigations performed prior to the development of the grouting base design include drilling of two medium deep boreholes, lithological analysis, geophysical surveying, hydraulic testing and thermal testing. Results used for characterizing the hydrogeological conditions at the site are presented and discussed in this section. Table 3-5 shows the activities and the borehole intervals for which data is available. Not included here are heat tracing test results since no significant

vertical flow could be detected. Borehole video logs were also collected but are not presented here.

Table 3-5. Details of borehole investigations. All depths refer to measured dept.

Activity	DH-BH1L	DH-BH2V
Hole deviation	3-300 m	3-244 m
ATV	3-300	3-133 m
Mechanical caliper	-	3-109 m
Single point resistance	15-300 m	17-244 m
Short normal resistivity	15-300 m	17-244 m
Long normal resistivity	15-300 m	17-244 m
Natural gamma	15-300 m	17-244 m
Hydraulic tests (WLM)		
5 m double packer	19.5-24.5 m 24.5-29.5 m 38-43 m 44-49 m	20-25 m 25-30 m 40.5-45.5 m 47.5-52.5 m 83-88 m
50 m double packer	11.2 - 61.2 m 61.2-111.2 m 111.2- 161.2 m 161.2-211.2 m 211.2 -261.2 m	14-64 m 64 -114 m 115-165 m 165-215 m
Single packer	211.2-300.0	165-244 m 8-244 m
Thermal tests (DTS during thermal recovery of DTRT)	0-300 m	52-242 m 0-190 m

Figure 3-5 shows a summary of some of the geophysical and thermal logs recorded in DH-BH1L (blue curves) and DH-BH2V (red curves) along the entire lengths of the boreholes. Reference depths are reported with respect to true vertical depth (TVD) calculated using the minimal curvature method. The combined ATV, mechanical caliper and electrical logs indicate relatively high degree of fracturing in the uppermost part of the rock mass down to a depth of approximately 60 m. At greater depths, the fracture intensity decreases, and anomalies detected from the normal resistivity logs can be contributed to isolated single or small groups of fractures. Also, anomalies in electrical log data for DH-BH2V appear as wider and larger in magnitude than for DH-BH1L, and less correlation is found between the log data sets. This may be explained since the horizontal distance between the boreholes starts to increase significantly at around 50 m depth.

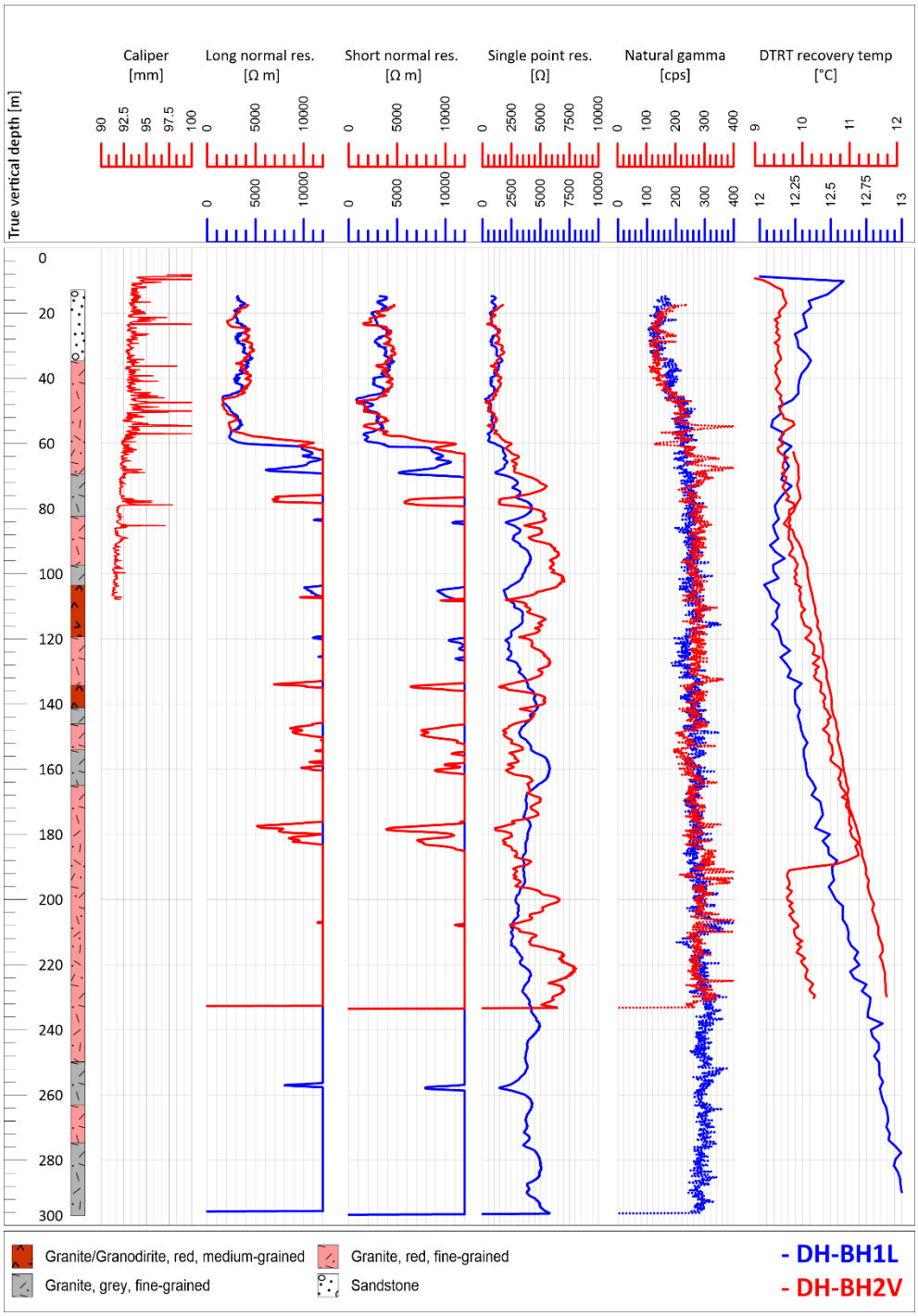

Figure 3-5. Lithology, mechanical caliper, electrical resistivity (long normal, short normal) and resistance (single point), natural gamma, and temperature profiles measured using optical temperature sensors during the recovery phase of distributed thermal response tests.

The litholigical change from sedimentary rock to igneous rock at c. 35-40 m depth is seen as an increase in radioactivity levels from the natural gamma logs shown in Figure 3-5. At greater depths the gamma activity levels are rather homogeneous although some anomalies can be seen, especially in DH-BH2V. A possible indication of groundwater flow through fractures is seen by the presence of

anomalies of thermal recovery temperature in DH-BH1L at ~55 m depth. At around 85 m depth, another indication of groundwater flow is seen as a clear spike in one of the recovery temperature profiles recorded in DH-BH2V, though this anomaly cannot be seen in the second temperature profile record taken about six months later during another DTRT.

The bar chart in Figure 3-6 shows the complete set of results from the evaluation of hydraulic tests performed in DH-BH1L and DH-BH2V. Test section lengths and locations are indicated by the size and position of the bar on the vertical axis showing measured borehole depth. Transmissivity values are plotted on the horizontal axis. The 50 m test section transmissivity data range spans from 8.4E-07 m^2/s to 2.6E-05 m^2/s for DH-BH1L and from 3.3E-07 m^2/s to 1.0E-05 m^2/s for DH-BH2V. Both maxima are measured in the shallowest intervals in respective boreholes. It must be noted that water flowing from the casing was observed during injection in test section 11.2 - 61.2 m in DH-BH1L, indicating that the transmissivity is overestimated due to the section being hydraulically connected to the non-isolated upper part of the borehole. This was also observed during testing of sections 61.2-111.2 m and 44.0-49.0 m in DH-BH1L.

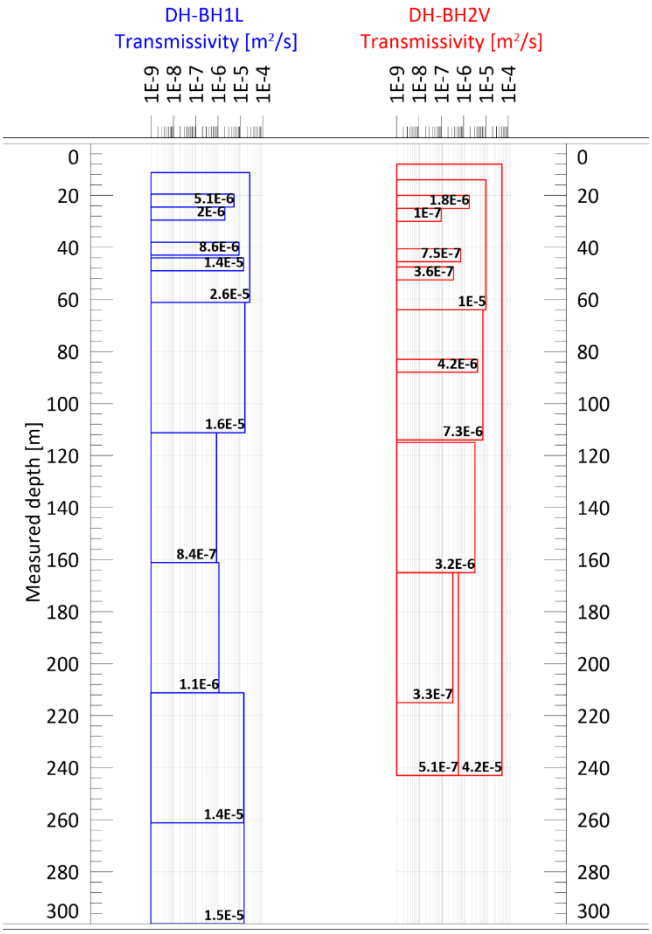

Figure 3-6. Summary of all hydraulic (WLM) tests conducted in boreholes DH-BH1L and DH-BH2V. Transmissivities are evaluated from tests with single packer and double packer setups with section lengths of 5 m and 50 m.

For both DH-BH1L and DH-BH2V estimated transmissivity values generally show a decreasing trend with depth, except for the transmissivities of the deepest sections of DH-BH1L (211.2-261.2 m and 211.2-300.0 m). The combined ATV and electrical logs indicate that the major contribution to the transmissivity of these sections is probably due to a single fracture located at c. 260 m depth.

Empirical cumulative distribution functions (ECDF) based on all transmissivity estimates with log-normal functions fitted to the ECDFs are depicted in Figure 3-7. The statistics indicate that DH-BH2V is less permeable but exhibit larger variance in transmissivity compared to DH-BH1L. The median transmissivity values for DH-BH1L and DH-BH2V are 1.1E-05 m²/s and 1.8E-06 m²/s, respectively.

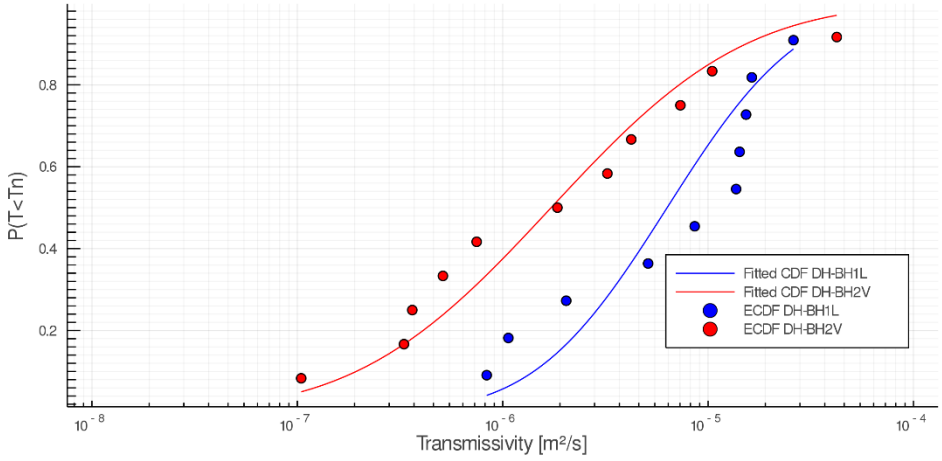

Figure 3-7. Empirical cumulative distribution functions (ECDF) with fitted log-normal distributions based on hydraulic tests carried out in DH-BH1L and DH-BH2V. P(T<Tn) represents the probability of a transmissivity estimate T being less than a or equal to a certain value (Tn). ECDFs are calculated using the Weibull formula (Gustafson 2009).

A summary of statistical measures for the hydraulic test results is given in Table 3-6.

Table 3-6. Basic statistics of hydraulic test results.

	DH-BH1L			DH-BH2V		
	5 m	**≥ 50 m**	**Total**	**5 m**	**≥ 50 m**	**Total**
No. of estimates	4	6	10	5	6	11
Median T [m²/s]	6.9E-06	1.4E-05	1.1E-05	7.5E-7	5.3E-6	1.8E-6
Mean T [m²/s]	7.5E-06	1.2E-05	1.0E-5	1.5E-6	1.1E-5	6.5E-6
Max. T [m²/s]	1.4E-6	2.6E-05	2.6E-05	1.8E-6	4.2E-5	4.2E-5
Min. T [m²/s]	2.0E-6	8.4E-07	8.4E-07	1.0E-7	3.3E-07	1.0E-7
Sum of T, ∑T [m²/s]	3.0E-5	7.3E-05	1.0E-4	7.3E-6	6.4E-5	7.1E-5
Sum of section lengths, ∑L [m]	20	338.8	358.8	25	513	538
∑T /∑L [m/s]	1.5E-6	2.2E-7	2.9E-7	2.9E-7	1.25E-7	1.3E-7

Based on the pre-investigations, it was decided to modify the original aim of performing grouting experiments along the entire length of the boreholes. Instead, the focus was shifted to the uppermost borehole sections in the interval 10-60 m below top of casing in order to limit the extent of the field work. Although a total of only 8 hydraulic tests were carried out with 5 m test sections at these depths, it was decided to not perform any complementary tests during the pre-investigation stage. Despite the small number of test data, fracture transmissivity distributions were estimated based on results of tests carried out in 5 m sections and lineal fracture intensities (Figure 3-8) interpreted from ATV logs.

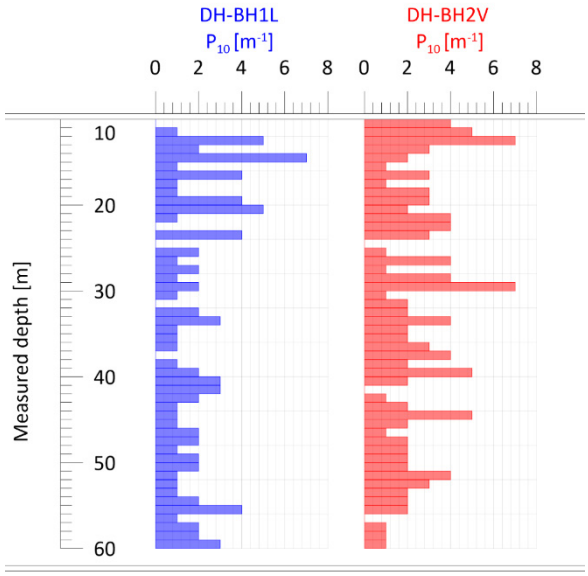

Figure 3-8. Lineal fracture intensity, P_{10}, in the interval 0-60 m.

Estimated fracture transmissivity distributions and corresponding fracture aperture distributions are presented in Section 3.6 below.

3.6 ESTIMATION OF FRACTURE TRANSMISSIVITY DISTRIBUTIONS

Following the approach described in Section 2.1, fracture transmissivity distributions and fracture aperture distributions were estimated using a calculation tool for rock characterization developed by (Thörn et al. 2015). A log-log CDF plot showing a Pareto distribution fitted to an empirical CDF based on fracture transmissivity data from DH-BH1L is presented in Figure 3-9. Calculated fracture hydraulic apertures corresponding to the Pareto distribution are also shown.

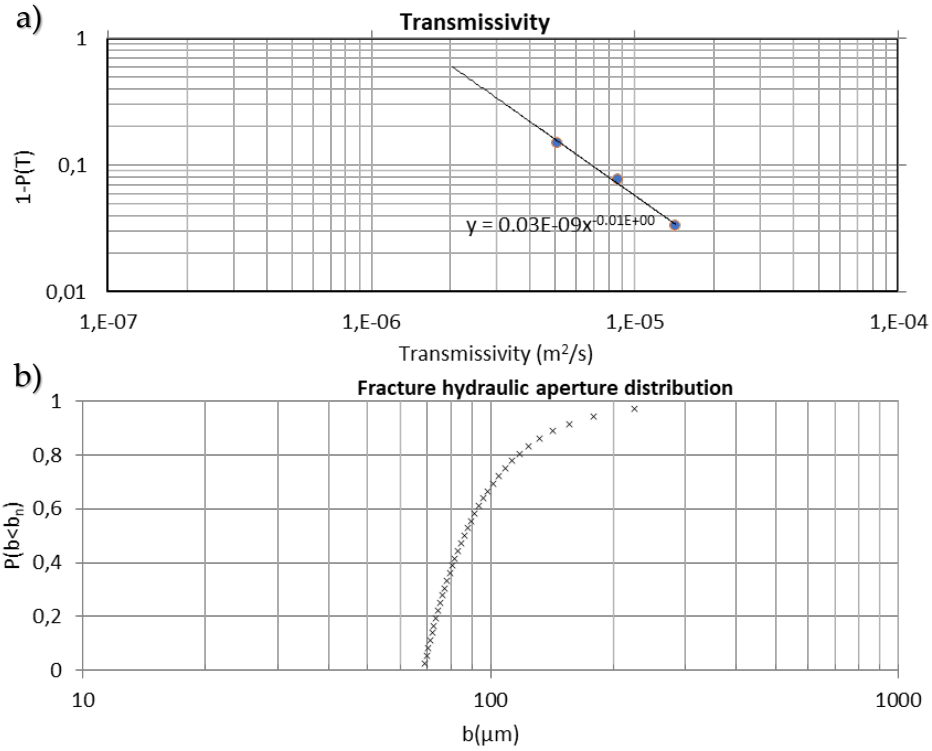

Figure 3-9. a) Fitting of a Pareto distribution to an empirical cumulative distribution function based on fracture transmissivity data from DH-BH1L. b) Calculated distribution of hydraulic fracture apertures.

According to the fracture distribution, the largest fracture aperture is 226 µm. This fracture can be expected to be located in a section with high transmissivity and a low number of fractures, that is section 44-49 m in DH-BH1L. By using the cubic law and the interval transmissivity value of the test section, the cumulative (total) fracture aperture can be estimated to be around 283 µm. That is, the largest fracture in the interval corresponds to 80% of the cumulative fracture aperture according to this estimation. Assuming that this relationship also applies to the remaining test sections, the largest estimated fracture apartures in each section can be calculated from their corresponding hydraulic test results (Table 3-7).

Table 3-7. Estimated maximum hydraulic fractures in test sections.

Section	Flow rate (l/min) at 200 kPa	Hydraulic fracture aperture	
		Cumulative b_{tot}	Maximum b_{max} (80% of b_{tot})
DH-BH1L 19.5-24.5 m	8.2	201	161
DH-BH1L 24.5 -29.5 m	3.3	148	118
DH-BH1L 38.0-43.0 m	13.9	239	191
DH-BH1L 44.0-49.0 m	22.9	283	226

Estimates of hydraulic fracture aperture provide useful information in grouting design when predicting grout penetrability and penetration lengths of the grout. It

should be noted that in this case the estimates were considered uncertain because of difficulties in interpreting fracture characteristics from ATV logs and lack of hydraulic data. They were however used as indicative values when establishing the grouting design prior to the field experiments. For a more detailed characterization fracture mapping from core-drilled boreholes should ideally be performed, which has not been possible in this case.

4 Grouting design methodology

In this section, a design methodology and procedure for fracture grouting as well as post-grouting evacuation and hydraulic testing of borehole sections is presented. A description of the design work and planning conducted prior to the grouting field experiments is also given.

For the application dealt with in this study, the intented purpose of employing grouting is to obtain suitable conditions for fluid circulation in open-hole borehole heat exchangers with minimal fluid losses into the formation. Such conditions could possibly be achieved by 1) sealing of fractures in boreholes whose only purpose is for grouting, for reducing the overall transmissivity of the rock mass at the heat storage site, 2) sealing of fractures by grouting in boreholes also intended for heat exchange (i.e. BHEs), and hence creating grout plumes surrounding the BHE itself or 3) a combination thereof. The second option is of primary focus in this study because higher sealing efficiencies and less material usage could possibly be achieved since it allows for design and control of the grouting process with respect to the grouted borehole itself. Considering that borehole fields for BTES applications normally are very densely populated, option 2) could also have the same effect on the overall transmissivity as option 1).

The outline of requirements that were stated in the initial phase of the design process is given below. The requirements were stated considering the objectives of the study, the extent of the field work as well as the feasability of future large-scale implementations.

- Efficient and durable sealing of fractures.
- Possibility to perform post-grouting hydraulic tests for investigating borehole tightness without requiring re-drilling.
- Fast grouting process (including post-grouting hydraulic tests) with little material usage.

The above-mentioned requirements imply, in brief, that any grout residing in the grouting section must be evacuated before the grout has hardened too much. This agrees with the requirement of a fast grouting process with subsequent hydraulic testing, which makes the field experiment procedure more time efficient and could also enable efficient grouting-while-drilling applications for large-scale implementations in the future. To achieve an efficient and durable grouting result, care must however be taken to ensure proper penetration and to prevent mechanical breakdown of the grout during and after grouting (see Section 2.2.2 and Section 2.2.3). Penetration length, material strength development and test section pressure during post-grouting testing are all crucial design parameters that must be taken into consideration.

4.1 GENERAL DESCRIPTION OF GROUTING AND HYDRAULIC TESTING PROCEDURE

The testing plan for investigation of sealing efficiencies achieved with respect to the grouted borehole section itself can briefly be summarized as follows:

1. Pre-grouting hydraulic testing.
2. Grout filling and grouting.
3. Evacuation of grout from borehole section.
4. Post-grouting hydraulic testing.

Sealing efficiencies are evaluated with regard to the results of the pre-grouting and post-grouting hydraulic tests. Hydraulic tests and grouting are performed using a double packer setup. For the field experiments carried out in this work a section length of 3.35 m was chosen. The hydraulic tests performed include water loss measurements in all grouted sections before and after grouting, as well as pressure build-up tests in selected intervals for characterization of flow dimensionality before grouting.

The pre-grouting hydraulic test in the grout section is used as basis for grout selection. Cement-based grouts are used for fractures with estimated hydraulic apertures larger than ~100 μm. Silica sol is used for sealing of narrower fractures due to the limited penetrability of cementitious grouts (Fransson, Funehag, and Thörn 2016). For the test plan that was developed prior to the grouting field experiments, preliminary grout selections were made based on the estimated fracture aperture distributions found in the pre-investigation stage.

4.2 TIGHTNESS CONDITIONS AND REQUIREMENTS

No specific tightness requirement has been defined in terms of transmissivity or fluid loss during hydraulic testing etc. Although an important consideration, the overall borehole tightness required to ensure satisfactory hydraulic performance and smooth operation of full-scale open-hole BHEs is site specific and has not been within the scope of this study. Instead, the aim here was to achieve an observable sealing effect of the grout and to ensure that the sealing effect remained even after pressure loading on the grout plume by post-grouting hydraulic testing. The design hydraulic head, i.e. the minimum section head that must be withstood without observing decreased sealing effect during hydraulic testing, was set to ~10 mH_2O (0.1 MPa).

4.3 GROUTING DESIGN BASED ON PENETRATION LENGTH AND MATERIAL STRENGTH DEVELOPMENT

The grouting design presented here is based on research on grout penetration and mechanisms causing mechanical breakdown of grouts in fractures. These topics are briefly dealt with in Section 2.2.

As described in Section 2.2.2, calculation of grout penetration demands knowledge of rheological properties (viscosity, yield stress, gel induction time) of the grout as well as fracture characteristics (aperture, geometry). If the fracture characteristics are known, the rheological properties and the grouting pressure and time can be controlled to achieve a certain penetration length given a specific fracture aperture.

When performing post-grouting hydraulic tests in the grouting section, a hydraulic gradient over the grout plume will be induced. To avoid erosion of the fresh grout due to high section pressure, the yield stress must be larger than shear stresses

exerted on the grout, as was shown in Section 2.2.3. The magnitude of the shear stress depends on the combination of section pressure, penetration length and the fracture aperture while the yield stress depends on the strength development of the grout after grouting. Hence the penetration length, grout strength development and post-grouting section pressure are all relevant parameters that should be incorporated in the design.

4.3.1 Penetration length

There are various combinations of parameter values that can be chosen to fulfill design criteria. In this case the minimum required penetration length was set to 2.5 m, which corresponds to the distance between DH-BH1L and DH-BH2V at ground surface level.

Cement-based grouts are intented for sealing of fractures with hydraulic apertures larger than ~100 µm. Figure 4-1 shows the penetration of a cement-based grout in fractures with two different hydraulic apertures as a function of grouting time, calculated following the approach described in Section 2.2.2. In this example only 2.5-5 minutes effective grouting time is needed to achieve the required penetration length.

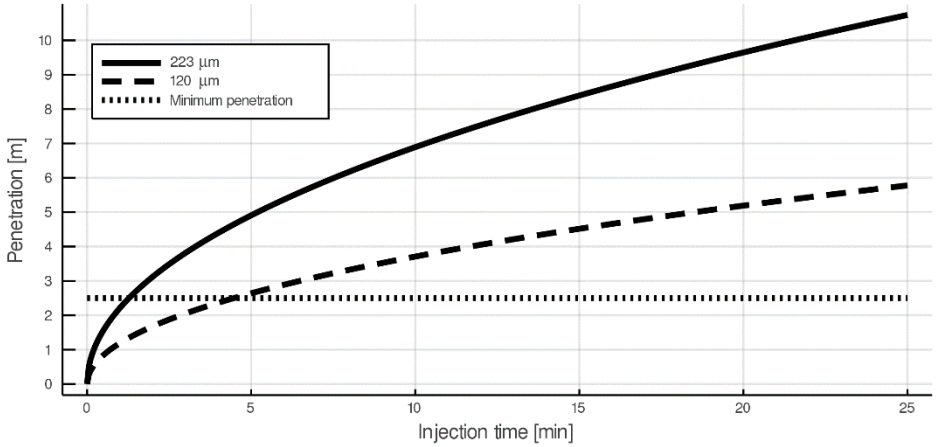

Figure 4-1. Penetration of a cement-based grout (µ = 25 mPas, τ_0=2 Pa) in fractures with hydraulic apertures 120 µm and 223 µm as a function of time, using a grouting pressure of Δp = 1.5 MPa.

Fractures narrower than ~100 µm are sealed using silica sol. The penetration of silica sol is governed by the gel induction time of the grout (see Section 2.2.1 and Section 2.2.2). An example showing the penetration of a gelling silica sol with gel time = 21 min (corresponding to a gel induction time of ~7 min) is shown in Figure 4-2. Penetration lengths of non-gelling silica sol are also shown for reference.

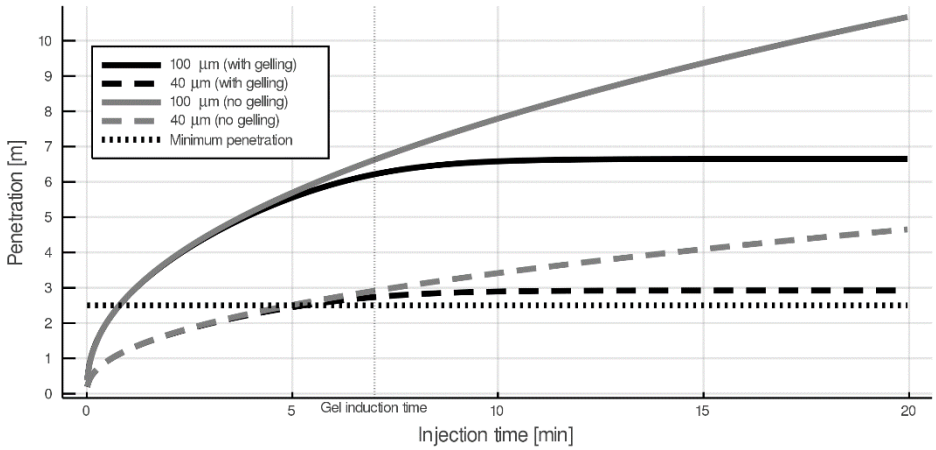

Figure 4-2. Penetration of silica sol with μ_o = 5 mPas, gel time =21 min and gel induction time = 7 min in fractures with hydraulic apertures of 100 µm (black solid curve) and 40 µm (black dashed curve), using a grouting pressure of Δp = 1.5 MPa.

Apparently, the penetration length in the wider fracture is more than twice as large as in the narrower fracture at gel induction time. Figure 4-2 also imply that higher grouting pressure or longer grouting/gel induction times might be needed in case sealing of even narrower fractures (e.g. ~10 µm) is required.

4.3.2 Stop criteria

A stop criterion based on shear strength of the grout is employed in order to avoid erosion or back-flow during hydraulic testing in recently grouted sections. The grout must harden to a specific strength before pressurizing the grouted section with water. By combining the relationship between grouting time and penetration length with criteria for avoiding erosion during grouting with cement-based grouts (see Section 2.2.2 and 2.2.3), a design window for cement-based grouts can be produced (Figure 4-3). The criteria can be related to the relative penetration, and is not directly dependent on fracture aperture (Axelsson 2009).

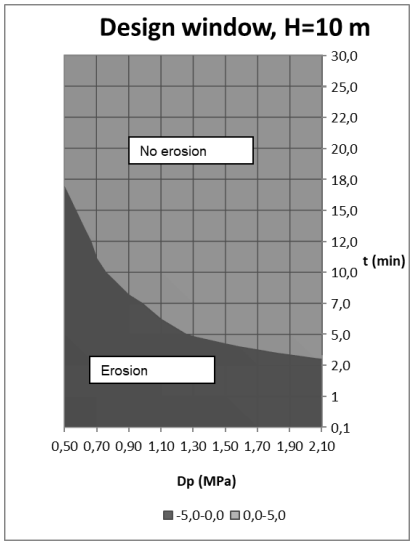

Figure 4-3. Design window for reducing the risk of erosion of a cement-based grout with viscosity μ = 30 mPas and yield stress τ_0=2 Pa. A water pressure of 10 mH_20 is acting on the grout plume. Modified from (Funehag 2017).

The pressure is in this case due to post-grouting water injection, but the criteria shown in Figure 4-3 also apply to situations where natural hydraulic gradients act on the grout during grouting.

As described in 2.2.3, the shear strength of the grout must be sufficiently high to balance the shear stress from the water in order to avoid erosion of the grout. The minimum required yield stress of the grout is dependent on fracture aperture and hydraulic gradient across the grout plume, as shown in Figure 4-4.

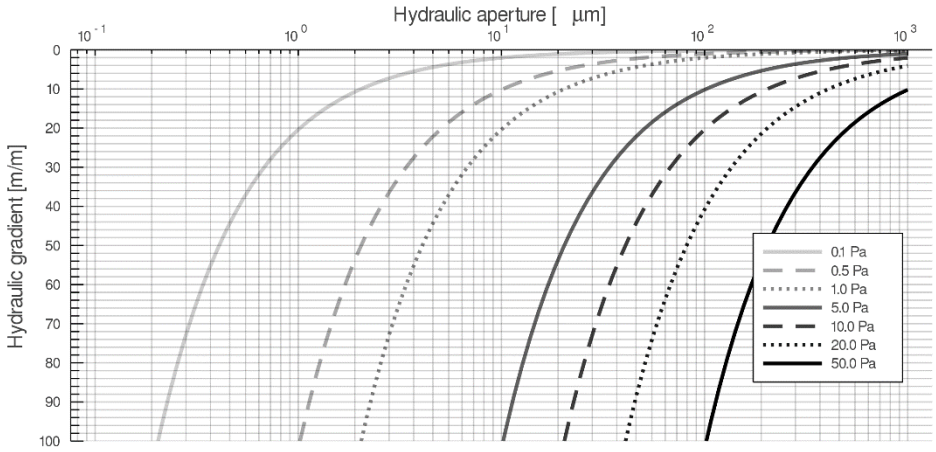

Figure 4-4. Minimum yield stress required for avoiding erosion of the grout, as a function of hydraulic gradient and aperture.

The hydraulic gradient resulting from the water injection tests depends on the section pressure and penetration length, as can be seen in Figure 4-5. See subsection 2.2.3 for reference.

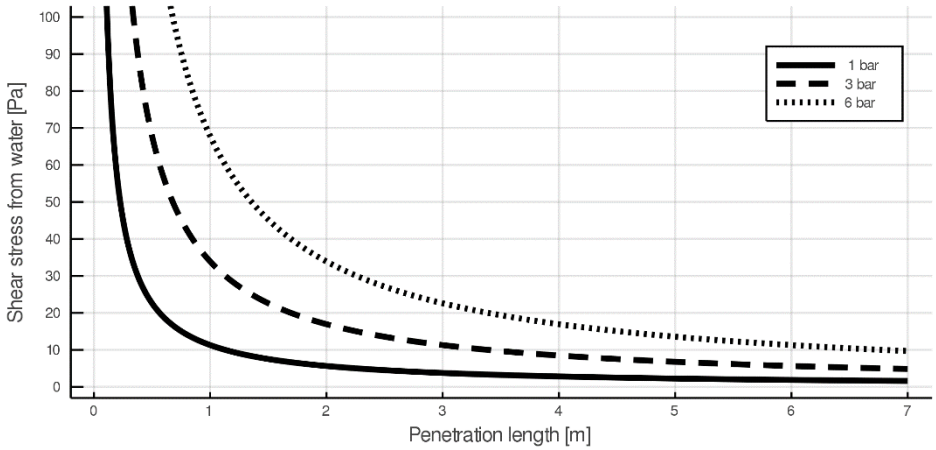

Figure 4-5. Shear stress from water as a function of penetration length for various injection pressures after grouting of a fracture with hydraulic aperture 226 µm.

Using the relationships described above, a grouting design based on penetration length, fracture aperture, water injection pressure and grout material strength can be developed. The grouting will continue until at least the minimum required yield stress of the grout has been achieved. Considering a water injection pressure of 0.1 MPa and a penetration length of 2.5 m in a fracture with hydraulic aperture of 226 µm, a shear strength of ~4 Pa would be required to avoid back-flow. The open boreholes adjacent to the grouting borehole may however reduce the penetration length in certain directions, and hence cause local regions of higher shear stress in the grout. Therefore, the required shear strength of cement developed at the end of the grouting process was set to 10 Pa. For silica sol grouting, the time criteria for stopping the grout pump and deflating the lower packer were set at a minimum of 4/5 and 1/1 of gel time, respectively. At gel time, the shear strength of silica sol is approximately 60-80 Pa (Funehag 2012).

4.4 DETAILED DESCRIPTION OF GROUTING AND HYDRAULIC TESTING PROCEDURE

A detailed description of the grouting and hydraulic testing procedure is given below. Figure 4-6 shows a schematic of the main steps involved in the procedure.

1. Inflation of upper and lower packers.
2. Performance of pre-grouting hydraulic test (WLM).
3. Grout selection based on WLM test result.
4. Preparation of grout and initial grout properties testing.
5. Grout filling and water evacuation using a low grouting pressure. Filling continues until twice the volume of the test section has been introduced, and grout is observed flowing from return tubings connected to the grout section.

6. Initial testing of grout samples collected from the evacuation tubings at the end of the filling process.
7. Grouting continues until stop criteria are met. Grout properties are tested at regular intervals during grouting.
    - Cement – 1.5 MPa grouting pressure set point. Pressure is maintained at a minimum of 15 minutes, until achieving a yield stress of at least 10 Pa.
    - Silica sol – 1.0 MPa grouting pressure set point. Gel time 21 minutes. Pressure is maintained until 4/5 of gel time.
8. Deflation of lower packer.
9. Grout evacuation by gravity and flushing water through grouting hose.
10. Inflation of lower packer.
11. Performance of post-grouting hydraulic test (WLM).

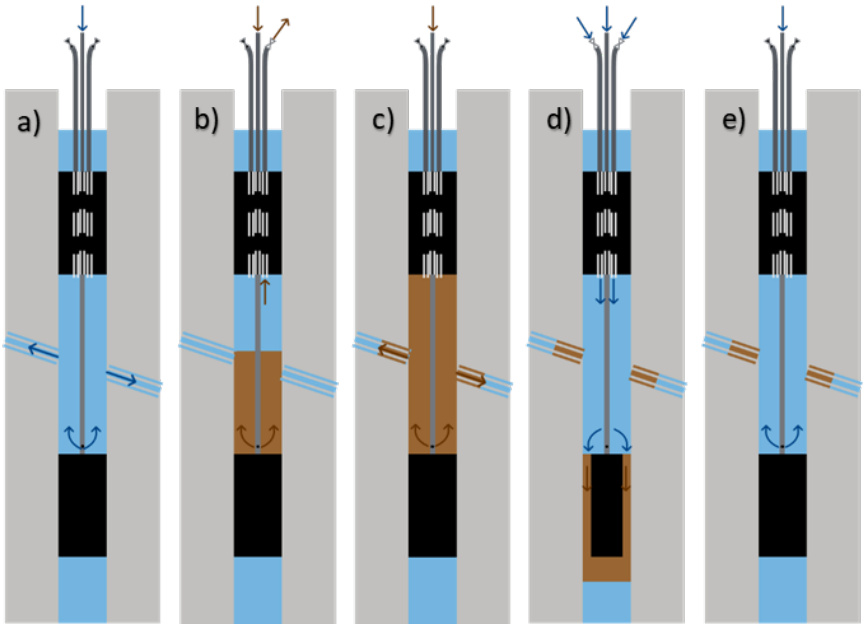

Figure 4-6. Schematic of the grouting and hydraulic testing procedure. Flow directions are indicated by arrows. a) Pre-grouting hydraulic test. b) Grout filling and water evacuation. Collection of grout samples via return tubings. c) Grouting. d) Grout evacuation. e) Post-grouting hydraulic test.

5 Grouting field experiments

Grouting field experiments were conducted September 16 – October 3, 2019. The experiments comprised hydraulic testing and grouting attempts in borehole DH-BH1L and DH-BH2V. The primary objectives of the field experiments was to 1) test the proposed methodology presented in Section 4 in field conditions using different grouts appropriate for sealing of both wide (>100 μm) and narrow fractures (<100 μm), 2) investigate the sealing effect of the grout by hydraulic testing, 3) investigate that the sealing effect remains even after pressure loading on the grout plume.

5.1 EQUIPMENT AND MATERIALS

5.1.1 Grouting equipment

Batch grouting (Cement/silica sol)

The unit used for batch grouting was Häny IC grout plant comprising high shear mixer, agitator and grout pump. The unit can be used for preparation and grouting of cement-based grouts and silica sol mixes.

Parallel pumping unit for continuous mixing of silica sol and saline solution

A pumping unit developed by GMA AB was used for grouting with silica sol. The unit is using two pumps operating in parallel for continuous mixing of silica sol and saline solution with varying, pre-defined mixing ratio throughout the grouting process. Hence, it is possible to achieve simultaneous gelling of the silica sol without needing to prepare large batches contributing to high material waste.

5.1.2 Inhole equipment

A custom-built double-packer system with a test section length of 3.35 m was used. The upper packer is equiped with two extra tubings allowing for return-flow and evacuation of water and grout from the grout section. The tubings served several purposes: for enabling observation of the grout filling process, for enabling collection and testing of grout samples taken from the grout section, and for evacuating water from the section by means of injecting compressed air in order to reduce mixing between grout and water.

5.1.3 Hydraulic testing equipment

Water loss measurements were performed using a flow meter device with a lower measurement limit of 0.17 l/min (accuracy ± 5 %). A lower measurement limit of 0.083 l/min was stipulated for the measurements where no flow could be detected after grouting (grouted sections only), which is the upper value of the range of non-detectable flow rates specified for the flow meter.

5.1.4 Grouting materials and grout properties testing equipment

The grouting material used for cement grouting was Sika Injektering 30 (d_{95} = 30 µm). Cement grout additives available were Sika iAcc-1 (accelerator) and Sika iFlow-1 (dispersion admixture). The material used for silica sol grouting was silica sol solution (SiO_2 40 wt%, Levasil CB17) with saline solution (NaCl 10 wt%) as accelerator.

Field measurement equipments used for testing of properties of cement grouts are listed in Table 5-1. A comprehensive description of the measurement methods and the relationship between density, yield stress, funnel time and viscosity is given by (Fransson, Funehag, and Thörn 2016).

Table 5-1. Measurement equipment used in field for testing of cement grout properties.

Equipment	Property
Mudbalance	Density
Marsh funnel	Funnel time
Yield stick	Yield stress
Fall-cone	Shear strength
Filter pump (100 µm mesh)	Filtration stability

Beaker tests were carried out to determine required mixing ratios of silica sol/saline solution to obtain desired gel times of the grout, according to the procedure described by (Funehag 2012).

Two different grout recipes were used for the cement grout mixes (Table 5-2). Pre-testing of the grout mixes were carried out in field, including measurements of density, funnel time, filtration stability as well as yield stress and shear strength development. Measurements of density, funnel time and yield stress were also carried out prior to and during grouting.

Table 5-2. Recipes used for preparation of cement-based grouts.

Recipe	w/c-ratio	Additive	Mixing time
C1	0.8	-	90 s
C2	0.8	3.2% iAcc-1 by weight of cement	90 s

The results of the pre-tests done for Recipe C1 are given in Table 5-3 and Figure 5-1.

Table 5-3. Recipe C1: Injektering 30, w/c-ratio 0.8, no additives.

Equipment	Property	Value
Mudbalance	Density	1.58 kg/dm^3
Marsh funnel	Funnel time	36.5 s (1 l)
Yield stick	Initial yield stress	4 Pa
Filter pump (100 µm mesh)	Filtration stability	300 ml

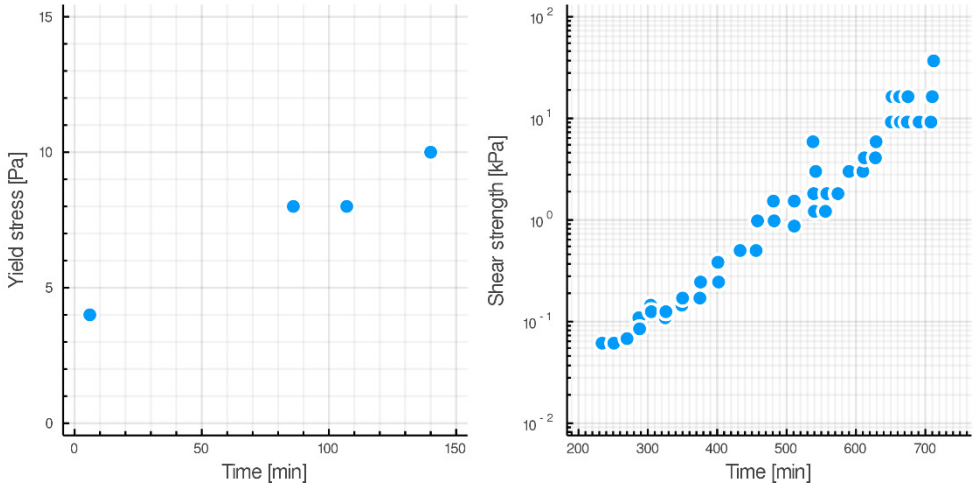

Figure 5-1. Recipe C1: Yield stress and shear strength as a function of time elapsed since end of grout preparation.

The results of the pre-tests done for Recipe C2 are given in Table 5-4 and Figure 5-2.

Table 5-4. Recipe C2: Injektering 30, w/c-ratio 0.8, 3.2% iAcc-1 by weight of cement.

Equipment	Property	Value
Mudbalance	Density	1,59 kg/dm^3
Marsh funnel	Funnel time	36 s (1 l)
Yield stick	Initial yield stress	1 Pa
Filter pump (100 µm mesh)	Filtration stability	300 ml

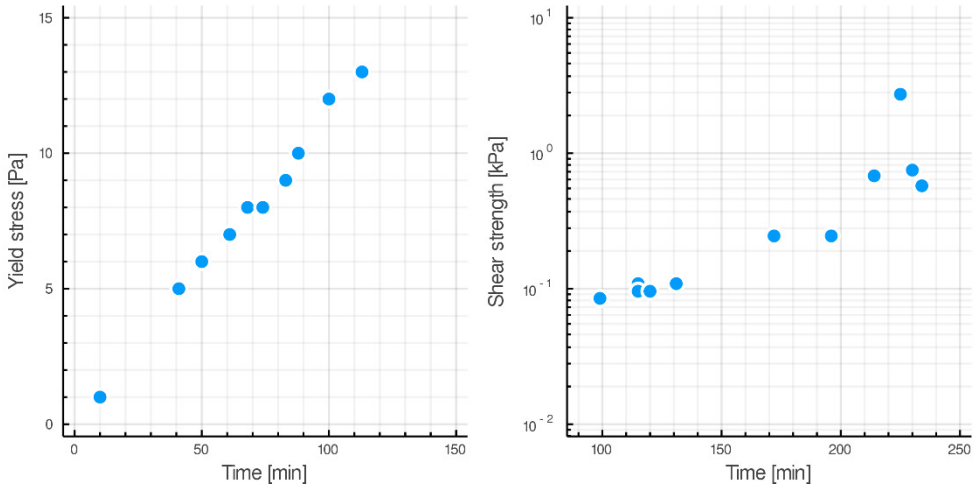

Figure 5-2. Recipe C2: Yield stress and shear strength as a function of time elapsed since end of grout preparation.

5.2 IMPLEMENTATION

Field experiments, including hydraulic tests (short-duration water loss measurements) and grouting attempts, were carried out mainly in the depth interval 10-60 m in boreholes DH-BH1L and DH-BH2V. An overview of the activities performed is shown in Figure 5-3. Borehole ID, size and position of the

test sections as well as activity type are indicated in the figure. Activities are arranged according to their chronological order.

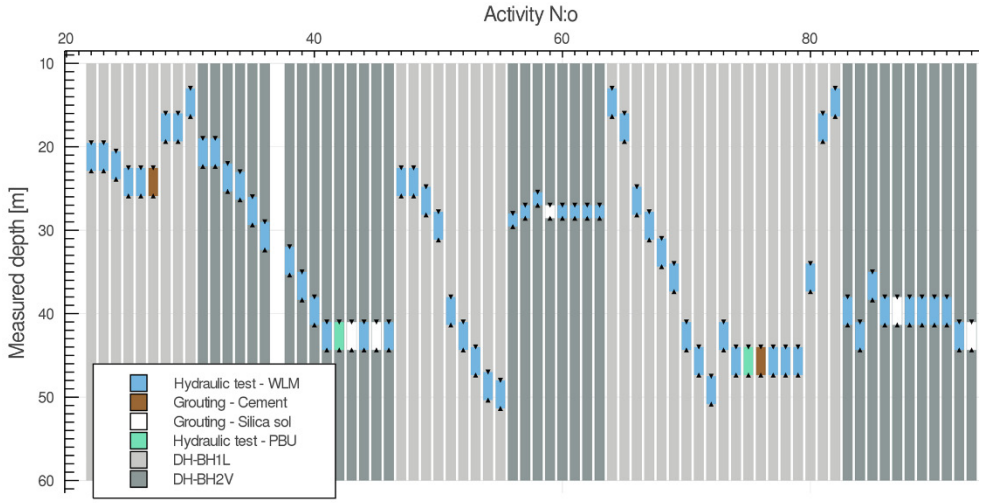

Figure 5-3. Overview of activities performed in the field work conducted during 16 September – 3 October 2019. The work comprised water loss measurements (WLM), pressure build-up (PBU) testing, and grouting using cement and silica sol grouts.

A total of eight grouting attempts were made in five different borehole sections. In addition to the attempts indicated in Figure 5-3, another attempt using cement-based grout was performed in section 83.00-86.35 m in borehole DH-BH2V. A summary of the grouting activities is presented in Table 5-5. Three attempts, using both cement-based grout and solica sol, could be performed essentially in accordance with the procedure described in Section 4.4. In one case, post-grouting hydraulic tests could not be accomplished immediately after grouting due to equipment failure, but the grouting result could eventually be investigated by hydraulic testing about 120 hours after grouting. The remaining four attempts were considered unsuccessful. Further details about the grouting attempts are given in the subsections below.

Table 5-5. Overview of grouting attempts listed in chronological order.

Date	Borehole ID	Section (m)	Grout	Comment
2019-09-19	DH-BH1L	22.53-25.88 m	Cement (Recipe C1)	Post-grouting testing could not be performed until 2019-09-24, sealing effect observed
2019-09-24	DH-BH2V	41.0-44.35 m	Silica sol	First attempt, no sealing effect observed, no gelling achieved during grouting
2019-09-24	DH-BH2V	41.0-44.35 m	Silica sol	Second attempt, no sealing effect observed, no gelling achieved during grouting
2019-09-25	DH-BH2V	27.0-28.56 m	Silica sol	Sealing effect observed
2019-09-30	DH-BH1L	44.0-47.35 m	Cement (Recipe C2)	Sealing effect observed
2019-10-01	DH-BH2V	38.0-41.35 m	Silica sol	Sealing effect observed
2019-10-01	DH-BH2V	41.0-44.35 m	Silica sol	Third attempt, disrupted due to pump failure
2019-10-02	DH-BH2V	83.0-86.35 m	Cement (Recipe C2)	Post-grouting testing could not be performed

5.2.1 Cement grouting

Three grouting attempts using cement-based grouts were made in test sections 22.53-25.88 m DH-BH1L, 44.0-47.35 m DH-BH1L and 83.00-86.35 m DH-BH2V.

The grouting of test section 22.53-25.88 m DH-BH1L essentially followed the design procedure, but the packers were stuck after it was decided to raise the packer because of difficulties encountered in flushing water through the grouting hose after grouting. The post-grouting hydraulic test failed because of an obstruction encountered at a depth of ~22-25 m when attempting to lower the packer again. The obstruction was eventually cleared on 2019-09-24, about 120 hours after grouting. No flow could be detected when performing WLM tests at pressures up to 0.3 MPa. Yield stress measurements were performed on grout samples taken from the return tubings at the end of the filling process. Measurements carried out 35 minutes and 3 minutes before opening the lower packer gave yield stress values of 9 Pa and 15 Pa, respectively.

Only one of the attempts, in test section 44.00-47.35 m DH-BH1L, could be performed in accordance with the planned procedure, including pre-grouting hydraulic testing, grouting and immediate post-grouting hydraulic testing. The grouting essentially followed the design described in Section 4.4, except that slightly lower grouting pressures (varying between 1.0-1.3 MPa) were employed. Yield stress tests were regularly carried out on a grout sample taken from the agitator immidiately after mixing of the first batch. Grouting continued until a yield stress of 10 Pa was reached, and the lower packer was opened within 8 minutes after pumping had ended. No detectable flow could be observed during post-grouting WLM tests performed at pressures up to 0.3 MPa.

A third attempt was made in section 83.00-86.35 m DH-BH2V. Once again problems were encountered when flushing the grouting hose after opening both packers, despite using pressures up to 1.3 MPa. No post-grouting hydraulic test could be performed due to inhole equipment failure and time constraints.

5.2.2 Silica sol grouting

Five grouting attemps using silica sol grout were made in test sections 27.00-28.56 m DH-BH2V, 38.00-41.35 m DH-BH2V and 41.00-44.35 m DH-BH2V.

Two grouting attempts on 2019-09-24, and an additional attempt on 2010-01-01 were made in test section 41.00-44.35 m DH-BH2V using the GMA mixing and pumping unit for silica sol grouting. All attempts failed because of problems with inadequate gelling due to possibly improper mixing ratios of silica sol and saline solution (1st and 2nd attempts) and pump failure (3rd attempt). Although a large amount of silica sol grout was injected into the rock during the first and second attempt, no sealing effects were observed during post-grouting hydraulic tests.

One grouting attempt was made in 27.00-28.56 m DH-BH2V. Batch grouting was performed using the Häny unit. Since large amounts of silica sol were wasted during the grouting attempts in test section 41.0-44.35 m in DH-BH2V, the aim was to minimize the material usage by shortening the double-packer section and grouting hoses. An attempt was made to minimize the amount of water in the

section by pushing the water downwards by compressed air injection through the grouting hose, and thereby preventing dilution of silica sol when filling the grout. Despite this effort, no gelling of the sample taken from the return tubing did occur during grouting. Gel time measured on samples taken from the agitator showed, however, good agreement with desired gel time, 30 minutes and 31 minutes respectively. Design grouting pressure of 1.0 MPa was reached within 3 minutes, and grouting continued for ~25 minutes. Pumping stopped and the lower packer was opened about 3 minutes prior to gelling. Post-grouting hydraulic tests were performed with water pressures up to 0.4 MPa with no detectable flow observed.

Another grouting attempt using the GMA unit was made in 38.00-41.35 m DH-BH2V. Desired gel time was set to 21 minutes after pump start. Again, actual gel times deviated from and exceeded desired gel times predominantly for the first 10 minutes of grouting. Better agreement was observed during the remaining time. Therefore, the procedure was repeated twice using a shorter gel time of 10 minutes in order to ensure proper gelling of the silica sol. The lower packer was opened after gelling occured. Post-grouting hydraulic tests were performed at water pressures up to 0.35 MPa with non-detectable flow. A flow rate above the lower measurement limit was eventually observed after increasing the pressure slightly to 0.41 MPa, which is most probably due to erosion of the grout caused by the large hydraulic gradient induced by pumping water into the test section.

5.3 FUTURE FIELD WORK

Hydraulic testing using an identical setup and method as was used for the tests carried out during the pre-investigation stage may be carried out for verifying the grouting results with higher accuracy of test equipment, and for direct comparisons between water loss rates obtained before and after completion of the grouting field experiments, respectively.

6 Results

In the field work, five borehole sections were grouted in a total of eight grouting attempts. In all cases the intention was to perform the grouting operation according to the proposed procedure involving evacuation of residing grout from the test section after grouting and immidiate post-grouting hydraulic testing. By pre- and post-grouting hydraulic testing the sealing efficiency of the grouting effort can be evaluated, upon which a decision can be made whether re-grouting is required. In this case, the aim of the experiments was to show that a sealing effect had been achieved by grouting, i.e. by observing a reduction in transmissivity after compared to before grouting, and to perform the post-grouting hydraulic tests at a minimum required pressure of 0.1 MPa without causing erosion and impairing the sealing effect thereof. The outcome is summarized below:

- **44.00-47.35 m DH-BH1L, 27.00-28.56 m DH-BH2V, 38.0-41.35 m DH-BH2V**

  Grouting and immediate post-hydraulic testing could be performed as intented. A durable reduction in transmissivity was observed during hydraulic testing with required pressure of 0.1 MPa. These attempts were made employing both cement-based grout and silica sol, respectively.

- **22.53-25.88 m DH-BH1L**

  Immediate post-grouting hydraulic testing could not be performed, but a reduction in transmissivity was observed at a later point.

- **41.00-44.35 m DH-BH2V (2 attempts)**

  Grouting and immediate post-hydraulic testing could be performed as intented, but no sealing effect was observed in the grouted section.

- **41.00-44.35 m DH-BH2V (1 attempt), 83.00-86.00 DH-BH2V**

  Post-grouting hydraulic tests could not be performed at all.

Hydraulic tests were performed also in non-grouted sections. These were evaluated with the aim of investigating possible tightening effects achieved in non-grouted sections by sealing of fractures that are hydraulically connected to grouted sections. Although the primary intention of the grouting was to seal the grouted section itself, the overall tightness of the boreholes is of interest when evaluating the grouting result.

All transmissivity estimates are evaluated from flow and pressure data obtained from water loss measurements. As described in subsection 5.1.3, the lower measurement limit is assumed to be 0.17 l/min for all flow measurements conducted in non-grouted sections. In post-grouting hydraulic tests in grouted sections, a lower limit of 0.083 l/min was assumed in the case of non-detectable flow. All values are evaluated using Moye's formula according to Equation (2-4).

6.1 GROUTED TEST SECTIONS

Results from the water loss measurements that were performed in tests sections where a sealing effect was observed after grouting, i.e. sections 22.53-25.88 m DH-BH1L, 44.00-47.35 m DH-BH1L, 27.00-28.56 m DH-BH2V and 38.0-41.35 m DH-BH2V, are presented in Figure 6-1. The figure depicts the chronological order and section location for the hydraulic tests as well as the grouting attempts performed in these sections. Tests carried out in one and the same section are indicated by connecting line segments in the transmissivity plot. Red crosses indicate transmissivity levels corresponding to the actual pressure and the lower measurement limit for flow. Transmissivity estimates corresponding to the case of non-detectable flow are indicated by black crosses.

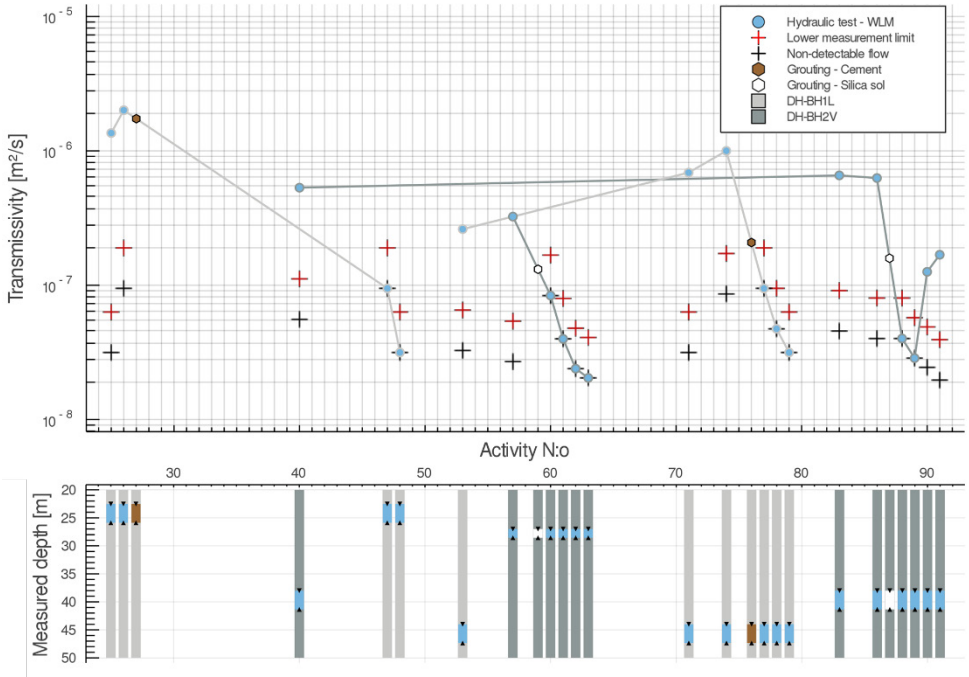

Figure 6-1. Results of pre- and post-grouting water loss measurements (WLM) carried out in grouted sections where a sealing effect was observed after grouting (22.53-25.88 m DH-BH1L, 44.00-47.35 m DH-BH1L, 27.00-28.56 m DH-BH2V and 38.0-41.35 m DH-BH2V).

As shown in Figure 6-1, post-grouting transmissivity estimates corresponding to non-detectable flow were obtained after all of these grouting attempts. Multiple post-grouting hydraulic tests were performed in sequence after each grouting attempt, with increasing water pressures starting from 0.1 MPa. Depending on the water pressure, transmissivity estimates range from 9.48E-8 m²/s (at 0.1 MPa) to 2.04E-8 m²/s (at 0.41 MPa) in the case of non-detectable flow. In section 38.00-41.35 DH-BH2V, flow rates above the measurement limit were eventually observed when increasing the water pressure to 0.41 MPa. This is possibly an indication that erosion of the grout occurred, resulting from high hydraulic gradients imposed during testing.

The sealing efficiencies of the grouting efforts are evaluated by comparing the minimum post-grouting transmissivity estimates ($T_{G,min}$) with the pre-grouting transmissivity estimates (T_0), according to $SE = 1 - T_G/T_0$. The results are summarized in Table 6-1.

Table 6-1. Pre- and post-grouting transmissivity estimates and sealing efficiencies achieved in test sections where a sealing effect was observed after grouting. All post-grouting transmissivity estimates are interpreted using a limit for non-detectable flow (NDF) equal to 0.083 l/min.

Borehole ID	Section (m)	Grout	T_0 (m²/s)	$T_{G,min}$ (m²/s)	Sealing efficiency (-)
DH-BH1L	22.53–25.88 m	Cement	2.01E-6	3.16E-8 (NDF, 0.3 MPa)	0.984
DH-BH2V	27.00–28.56 m	Silica sol	3.24E-7	2.04E-8 (NDF, 0.41 MPa)	0.937
DH-BH1L	44.00–47.35 m	Cement	1.00E-6	3.16E-8 (NDF, 0.3 MPa)	0.968
DH-BH2V	38.00–41.35 m	Silica sol	6.57E-7	2.87E-8 (NDF, 0.35 MPa)	0.956

6.2 NON-GROUTED TEST SECTIONS

A total of 63 water loss measurements were carried out in grouted and non-grouted test sections in boreholes DH-BH1L and DH-BH2V during the field work. Another 21 water loss measurements were performed in the pre-investigation stage. An overview of the results from the hydraulic tests carried out in short test sections (≤ 5 m) within the depth interval of 10 – 60 m is shown in Figure 6-2.

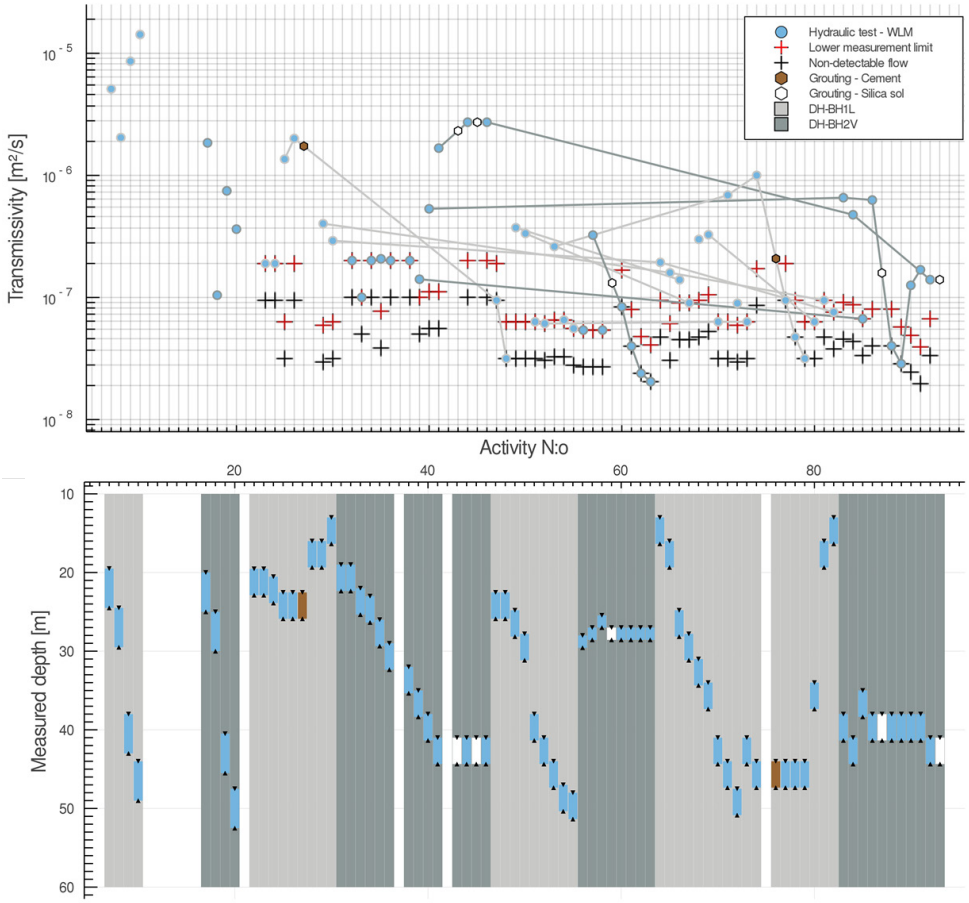

Figure 6-2. Overview of water loss measurements (WLM) and grouting attempts performed within the interval between 10–60 m in boreholes DH-BH1L and DH-BH2V.

Figure 6-3 shows the results from hydraulic tests carried out within the depth interval 18-32 m. Within this interval, transmissivity reductions in non-grouted sections were observed after both grouting attempts made in test sections 22.53-25.88 m DH-BH1L and 27.00-28.56 m DH-BH2V. In DH-BH1L, the estimates of transmissivity from pre-grouting hydraulic tests indicate the presence of a dominating fracture with an interpreted hydraulic aperture of ~130 µm located in the interval 23.88-24.50 m. After grouting in section 22.53-25.88 m DH-BH1L, transmissivity estimates from subsequent hydraulic testing at similar depths (19.00-26.35 m) in DH-BH2V were below the measurement limit, i.e. at least about one order of magnitude smaller than was obtained in section 20.00-25.00 m in the pre-investigation stage. After the grouting attempt in 27.00-28.56 m DH-BH2V, a flow rate above the measurement limit was observed in only one of the test sections in both boreholes. Overall, the maximum transmissivity estimate obtained within the considered depth interval was reduced from 5.1E-6 m²/s to 2.0E-7 m²/s (corresponding to the measurement limit for flow at a pressure of 0.1 MPa).

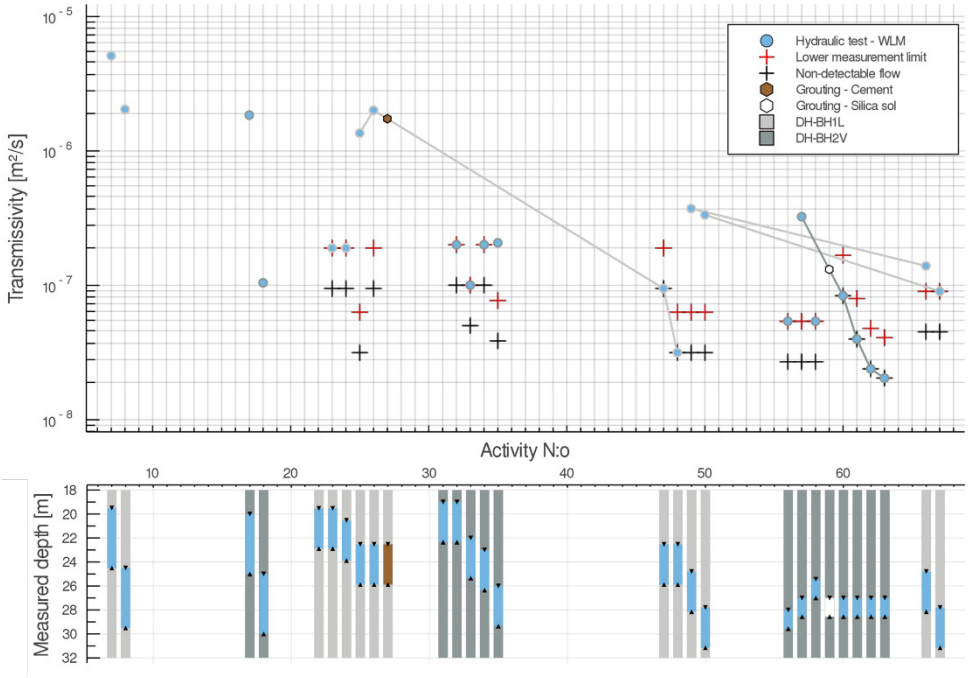

Figure 6-3. Results of the water loss measurements (WLM) carried out within the depth interval 18-32 m.

Results from hydraulic tests performed within the interval between 35-53 m are shown in Figure 6-4. Two failed grouting attempts were initially made in test section 41.00-44.35 m DH-BH2V. Although these attempts did not provide any sealing effect in the grouted section, a decrease in transmissivity was observed in comparisons between estimates obtained in the pre-investigation stage with post-grouting estimates in sections within the interval 38-49 m in DH-BH1L. After the respective grouting attempts made in sections 44.00-47.35 m DH-BH1L and 38.00-41.35 DH-BH2V, a gradual decrease in transmissivity was however achieved in 41.00-44.35 m DH-BH2V.

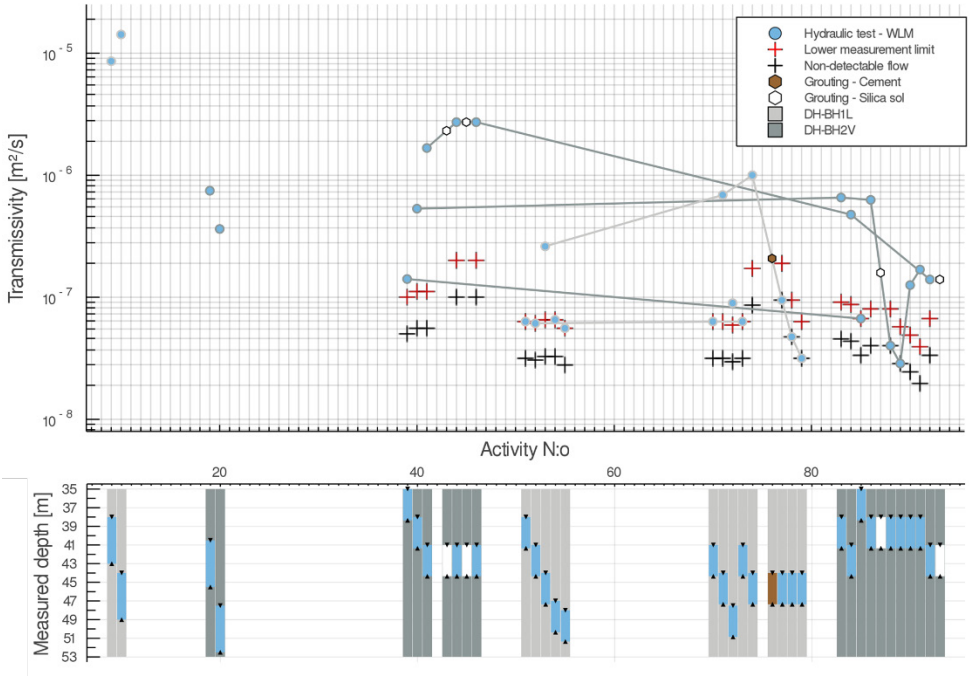

Figure 6-4. Results of the water loss measurements (WLM) carried out within the depth interval 35-53 m.

Excluding the results from the final hydraulic tests performed in the grouted sections 38.00-41.35 DH-BH2V and 41.00-44.35 m DH-BH2V, a reduction of the maximum transmissivity estimate from 1.4E-5 m²/s (section 44.00-49.00 m DH-BH1L) to 9.0E-8 m²/s (section 47.50-50.85 m DH-BH1L) was achieved within the depth interval 35-53 m in DH-BH1L. Note that no post-grouting hydraulic tests in the interval 44.35-53.00 m were carried out in DH-BH2V.

6.3 OVERALL BOREHOLE TIGHTNESS

Since the intervals of interest (i.e. primarily the sections tested in the pre-investigation stage) have not been investigated after completion of the grouting field experiments (see chapter 5), it is not possible to make a direct comparison between overall pre- and post-grouting transmissivity levels. Instead, a subset of the complete set of transmissivity estimates obtained in short sections (≤ 5 m) within the interval 10-60 m is evaluated. The set consists of estimates obtained from the last measurement carried out in each respective section, after the first grouting attempt was made. Estimates from measurements in sections tested only once are also included.

The estimates are plotted on an empirical cumulative distribution graph shown in Figure 6-5. As shown in the graph, all estimates except one are below or equal to 2.0E-7 m²/s, that is the level corresponding to the lower measurement limit for flow at a water pressure of 0.1 MPa. Lower levels of transmissivity were obtained by using higher pressures during some of the hydraulic tests, also indicated are the levels corresponding to the lower measurement limit and non-detectable flow at a pressure of 0.3 MPa. The estimates span from 2.0E-8 m²/s to 3.0E-7 m²/s, as compared to the range of estimates between 1.1E-7 m²/s to 1.4E-5 m²/s that was

obtained from tests carried out in 5 m test sections within the considered depth interval in the pre-investigation stage.

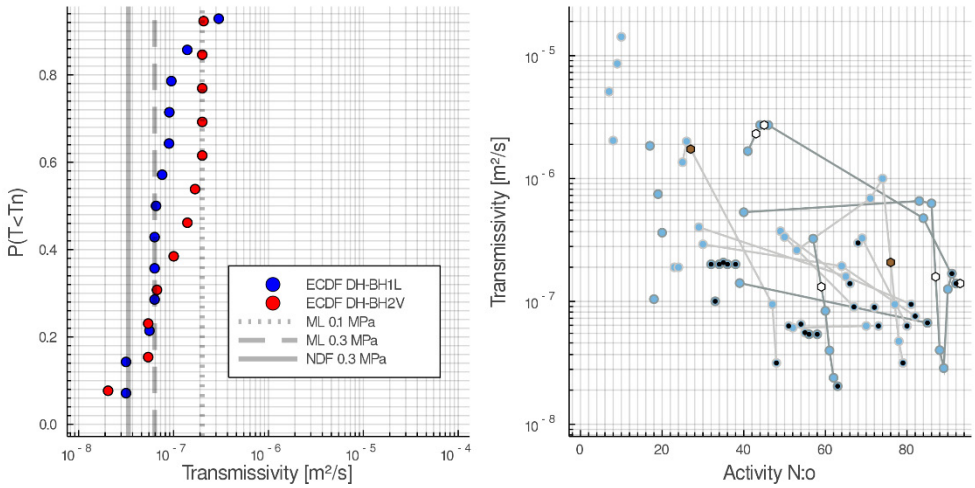

Figure 6-5. Empirical cumulative distribution function (left) based on a subset of transmissivity estimates indicated by black markers (right). Transmissivity values corresponding to lower measurement limit for flow (0.1 MPa and 0.3 MPa) and non-detectable flow (0.3 MPa) are shown. P(T<Tn) represents the probability of a transmissivity estimate T being less than a or equal to a certain value (Tn). ECDFs are calculated using the Weibull formula (Gustafson 2009).

Basic statistical measures for the set of estimates are shown in Table 6-2. The median and mean of the set are 9.0E-8 m²/s and 1.1E-7 m²/s, respectively. The sum of transmissivity estimates divided by the sum of section lengths is a measure of average hydraulic conductivity equivalent to that of an assumed homogeneous rock mass.

Table 6-2.

Measure	Value
No. of estimates	25
Median T [m²/s]	9.0E-8
Mean T [m²/s]	1.1E-7
Max. T [m²/s]	3.0E-7
Min. T [m²/s]	2.0E-8
Sum of T, ∑T [m²/s]	2.8E-6
Sum of section lengths, ∑L [m]	78
∑T /∑L [m/s]	3.5E-8

The resulting value of 3.5E-8 m/s is approximately one to two orders of magnitude less than similarly calculated values obtained from hydraulic tests performed in the pre-investigation stage, see Table 3-6 in subsection 3.5.

7 Discussion

This study has investigated the possibility in reducing or preventing loss of circulation in open-hole, pressurized boreholes. The study is intended as a first step in developing a coaxial, single-pipe borehole heat exchanger for HT-BTES applications in hard rock. It is assumed that the amount of fluid losses can be significantly reduced by sealing of fractures intersecting the borehole, considering that the rock matrix has insignificant porosity and that fluid flow predominantly occurs through interconnected secondary porosities such as fractures within the rock mass. For this purpose, fracture sealing by permeation grouting has been identified as a possible means to achieve required permeability of the borehole wall and the rock mass surrounding the borehole.

A major objective has been the development of a grouting design methodology and procedure to implement open, ideally impermable, boreholes in the field. Efforts were made to develop a procedure that enables a fast grouting process and subsequent re-opening of the grouted borehole section immidiately after grouting by evacuating the fresh grout by flushing with water. This way, the grouting process can be designed and performed as a selective measure considering those specific fractures that cause the loss of fluid. Further, grouting results can be controlled and evaluated with respect to tightness requirements by immidiate post-grouting hydraulic testing, thus permitting rapid decisions concerning need for re-grouting or proceeding with other sections. Other options, such as accomplishing an overall reduction of the rock mass permeability by injection via designated grout boreholes, would probably not be as reliable and efficient in terms of achieved sealing effect and grout material consumption.

The proposed grouting design methodology was developed with the aim of enabling the abovementioned procedure without causing risk of mechanical breakdown of the fresh grout due to post-grouting evacuation and hydraulic testing. With knowledge of the hydraulic apertures of fractures that need to be sealed to meet post-grouting water loss criteria at required pressure, a suitable grouting technique and grout material can be chosen to achieve desired grout spread and hydraulic gradient across the grout plume. Recent developments in the fields of fractured rock characterization, modeling of grout flow as well as grout rheology have made it possible to design grouting works by accurately predicting penetration and groutability in individual fractures (Gustafson and Stille 2005; Funehag and Gustafson 2008b; Fransson, Funehag, and Thörn 2016; Fransson 2008). Moreover, the strength development of the grout material can be observed by means of simple field measurements methods, thus allowing for precaution and control to prevent erosion of the grout during post-grouting events under practical conditions. Altogether, using existing theoretical and practical tools available, a methodology for grouting design based on penetration length, material strength development and post-grouting hydraulic testing pressure could be developed for both silica sol and cement-based grouts.

Small-scale grouting field experiments were carried out with the objective of demonstrate the proposed methodology under practical conditions. No specific tightness requirements were set, instead the aim was to achieve any durable

sealing effect after performing the grouting operation and post-grouting hydraulic testing in accordance with the planned design and procedure. As was shown in Section 6, this aim was fulfilled or partially fulfilled in four grouting attempts using both silica sol and cement-based grouts. Although a sealing effect was achieved after all these attempts, it has not been possible to determine the actual amount of water loss during post-grouting hydraulic tests because of the measurement limit for flow of the equipment used. Neither has it been possible to estimate the resulting grout spread and hydraulic apertures of individual grouted fractures. Lack of data regarding test section transmissivities and uncertainties in fracture intensity made it difficult to accurately predict fracture aperture distributions, which is an important consideration in grouting design and analysis of the results. Hence, additional hydraulic tests in grouted sections as well as future experiments may help to provide more detailed insight in the level of tightness that can be obtained.

Problems occasionally encountered were difficulties in flushing water through the grouting hose after grouting, which led to failure after two grouting attempts using cement. This is a possible indication of conflicting requirements of the grout in the fractures (high flow resistance) and the hose (low flow resistance), which should be considered in the design to enable post-grouting activities without requiring raising the downhole equipment for maintenance each time. In general, an upper strength criterion should be specified in the design in order to avoid downhole equipment failure and obstruction of the borehole. Another issue encountered was dilution of the grout due to mixing with water when filling the borehole section, despite attempting to minimize the amount of water by injecting compressed air into the section. Even though this did not affect the results, the measurements on grout samples taken from the return tubing generally did not provide useful information on strength development as was intented. Instead, measurements were carried out on samples taken from the grouting unit. In general, since prevention of erosion of the grout material in the fractures is an important consideration in the design, care must be taken to ensure that shear stresses and material strength are accurately estimated to avoid using excessively high safety factors. These aspects are dependent on several factors, including fracture apertures, groundwater pressure distribution, shape of the grout plumes, post-grouting water pressure, and shear strength of the grout in the fractures. With better knowledge of these parameters although they are difficult to measure directly, the design can be improved, and significant time savings can potentially be achieved.

Concerning the use of permeation grouting techniques as an active method for large-scale implementation of single-pipe BHEs for HT-BTES applications, the feasibility is highly dependent on those tightness requirements that must be met to ensure adequate hydraulic performance of the BHEs and stable operation of the system. Investigation and analysis regarding loss of circulation fluid as a function of borehole and ambient formation pressure, degree of borehole permeability etc. has not been within the scope of this study. Future research is needed to increase the understanding on the aspects. Nevertheless, the characteristics of the undisturbed rock mass, the level of tightness that can or must be obtained, and the efforts required to achieve that level are crucial considerations.

Recently, the use of fine-sealing material such as silica sol have enabled very high levels of sealing to be achieved. In tunneling projects, estimates of rock mass hydraulic conductivities as low as ~1E-11 m/s have been reported (Funehag and Emmelin 2011). In terms of hydraulic aperture, it has been shown that silica sol is capable of penetrating fractures at least as narrow as 10 µm (equivalent to a fracture transmissivity of ~5E-10 m²/s) (Funehag 2012). However, although these levels are possible to achieve, the efforts required to meet tightness criteria may become very extensive. Considering that fractures having an aperture above a critical threshold of b_{crit} ought to be sealed, the extent of required grouting operations will be highly dependent on the depth-frequency distributions and aperture distributions of hydraulically conductive fractures intersecting the borehole. In Swedish crystalline rocks, borehole investigations have shown that distributions of hydraulic apertures can be approximated by Pareto distributions (Gustafson and Fransson 2005), i.e. the set of fractures consists of a large portion of narrow fractures and few wide fractures (see subsection 3.6). Fracture apertures and frequency may also be depth dependent, though high variability can occur e.g. due to the presence of deformation zones (Olofsson et al. 2001). It is clear that for a scenario in which fracture frequency is high and b_{crit} is low, the number of fractures that has to be treated, and consequently the portion of the borehole, may become large and hence prohibitive.

In general, good knowledge and understanding of fracture characteristics is required for feasibility assessments, canditate site selection, as well as for grouting design and execution. Despite comprehensive site investigation campaigns, there are always uncertainties regarding predicting and quantifying the extent of required efforts, thus contributing to difficulties with estimations of time and investment for implementation. This is related to the inherent heterogeneity of fractured rock masses on different scales. For large-scale productions, systematic strategies would be needed for grouting operations and verification of grouting results in order to minimize time and material consumption required for implementation of the BHEs. For example, a technical solution involving regular hydraulic testing and grouting during drilling advancement would likely provide time efficiency and reliability benefits. Fast advancement could be achieved by performing grouting, hydraulic tests and grout evacuation according to the design approach/procedure described in this report. Using silica sol seems to be a promising option allowing for time- and sealing-efficient grouting, thanks to its good penetrability, controllable gel times and rapid increase in material strength after mixing. However, technical development in integrated drilling and grouting equipment is needed to enable such an approach to be used.

In this work, only active sealing methods in thermally undisturbed rock have been considered and applied. Future investigations may however focus on implementation and operation of the intended end-product, i.e. BHEs for HT-BTES systems, with respect to LCA and long-term performance under operating conditions. Possible processes induced by elevated and cyclic subsurface temperatures or other condition variations that might affect the grout sealing and overall rock mass tightness should be considered. For example, coupled mechanisms involving thermal, hydrologic, mechanical and chemical processes are likely to cause changes in permeability due to thermally induced rock stress

changes or by mineral precipitation (Lundström and Stille 1978; Jones and Detwiler 2016). Also, long-term durability and longevity of grouts under different thermal, chemical and mechanical conditions are important considerations (Gustafson, Hagström, and Abbas 2008; Holt 2008; Grandia et al. 2010; Piepho 1997). Especially for silica sol grouts there is however paucity in the literature on this topic area, and hence more research is needed to increase understanding on long-term effects (Pan et al. 2018; Sögaard, Funehag, and Abbas 2018; Funehag 2012).

8 Summary, conclusion and future work

Theoretical and experimental work has been carried out to investigate the application of permeation grouting techniques to reduce or prevent circulation losses when circulating a fluid under pressure through open-hole, single-pipe coaxial borehole heat exchangers intended for large-scale high temperature borehole thermal storage systems in hard, low-permeable rock. Coaxial borehole heat exchangers that are open to the rock and operates under positive head conditions could allow for improved thermal performance compared to existing borehole heat exchanger designs.

Penetration and sealing of hydraulically conductive fractures intersecting the borehole involves injecting grout material into packed-off borehole sections under pressure. In recent decades, developments in theory and practice in the field of grouting have made it possible to design and perform grouting works in an accurate manner, and attainable levels of sealing efficiency have been improving.

A method has been developed for grouting, grout evacuation and hydraulic testing in borehole sections. The aim was to enable a fast procedure involving sealing of intersecting fractures, re-opening of the borehole section and immediate post-grouting hydraulic testing without risking impairing the sealing effect. Evacuating the grout with flushing water before setting appears to be an efficient approach because re-drilling efforts would otherwise be required to be able to access the borehole.

The risk of erosion of the fresh grout should however be considered to ensure that the sealing effect remains after pressurizing the borehole section during evacuation and hydraulic testing. With existing theoretical tools and adequate fracture hydraulic data available, grout material, grouting and hydraulic testing parameters can be properly selected to avoid erosion.

Grouting field experiments were conducted to demonstrate the proposed procedure under practical conditions. It was shown that grouting, grout evacuation and post-grouting hydraulic testing could be performed in accordance with the proposed procedure. Using both silica sol and cement-based grouts, durable sealing effects were achieved without observing indications of erosion in several of the attempts, although opposite observations also were made when applying water pressures higher than design pressure in one of the attempts. It can be concluded that the proposed procedure can be employed for sealing of borehole walls and re-opening of grouted borehole sections, and that erosion of the grout in the fractures is an important consideration that should be accounted for in grouting design.

The level of tightness required to ensure satisfactory hydraulic performance and functional operation of open-hole, single-pipe BHE systems is unclear. Future investigation may focus on analyzing flow dynamics in open boreholes. The analysis should address how the rock mass characteristics and groundwater conditions impact circulation fluid loss rates under different operation conditions. The goal of such a study could be to provide guidance on tightness requirements,

and whether favorable hydrogeological conditions exist for possible large-scale implementations. This would serve as a basis for future feasibility studies, in which the extent of required grouting efforts and demands on sealing performance can be assessed.

9 References

Abelin, H., I. Neretnieks, S. Tunbrant, and L. Moreno. 1985. "Final Report of the Migration in a Single Fracture - Experimental Results and Evaluation." SKB-SP-TR--85-03. Swedish Nuclear Fuel and Waste Management Co. http://inis.iaea.org/Search/search.aspx?orig_q=RN:16077313.

Acuña, José. 2013. "Distributed Thermal Response Tests : New Insights on U-Pipe and Coaxial Heat Exchangers in Groundwater-Filled Boreholes." http://urn.kb.se/resolve?urn=urn:nbn:se:kth:diva-117746.

Alkiswani, Mutaz, and Claes Regander. 2019. "Säsongslagring Av Överskottsvärme Vid KVV Filborna, Helsingborg." presented at the Geoenergidagen 2019, Stockholm. http://media.geoenergicentrum.se/2019/10/2_3_CR_MA_HT-BTES-Filborna_GED2019.pdf.

Andersson, Helen. 1998. *Chemical Rock Grouting. An Experimental Study on Polyurethane Foams*. https://research.chalmers.se/en/publication/928.

Axelsson, Magnus. 2009. *Prevention of Erosion of Fresh Grout in Hard Rock*. https://research.chalmers.se/publication/84178.

Axelsson, Magnus, and Gunnar Gustafson. 2006. "A Robust Method to Determine the Shear Strength of Cement-Based Injection Grouts in the Field." *Tunnelling and Underground Space Technology* 21 (5): 499–503. https://doi.org/10.1016/j.tust.2005.08.011.

Banks, David, E. Rohr-Torp, and H. Skarphagen. 1994. "Groundwater Resources In Hard Rock; Experiences from The Hvaler Study, Southeastern Norway | SpringerLink." *Applied Hydrogeology* 2 (2): 33–42.

Bruce, Donald. 2012. *Specialty Construction Techniques for Dam and Levee Remediation*. CRC Press.

Bruce, Dr Donald A, Rudy Lyon, and Stefan Swartling. n.d. "AN INTRODUCTION TO WATER-POWERED DOWN-THE-HOLE DRILLING IN SPECIALTY GEOTECHNICAL CONSTRUCTION."

Butrón, Christian, Magnus Axelsson, and Gunnar Gustafson. 2009. "Silica Sol for Rock Grouting: Laboratory Testing of Strength, Fracture Behaviour and Hydraulic Conductivity." *Tunnelling and Underground Space Technology* 24 (6): 603–7. https://doi.org/10.1016/j.tust.2009.04.003.

Butron, Christian, Gunnar Gustafson, and Johan Funehag. 2008. "Grouting in the Nygård Tunnel: Pre-Grouting Design for Drip Sealing and Evaluation." https://research.chalmers.se/en/publication/67949.

Byegård, Johan, Eva Hakami, Calle Hjerne, Rune Nordqvist, Vladimir Cvetkovic, Henrik Drake, Eva-Lena Tullborg, and Anders Winberg. 2017. "TRUE-1 Completion – Final Report." TR-12-11. SKB.

Cabeza, Louisa F. 2015. *Advances in Thermal Energy Storage Systems. Methods and Applications*. Woodhead Publishing Series in Energy.

Carlsson, Leif, and Gunnar Gustafson. 1984. *Provpumpning som geohydrologisk undersökningsmetodik*. Stockholm: Statens råd för byggnadsforskning : Sv. byggtjänst (distr.).

Darcy, Henry. 1856. *Les Fontaines Publiques de La Ville de Dijon: Exposition et Application Des Principes a Suivre et Des Formules a Employer Dans Les Questions de Distribution d'eau; Ouvrage Terminé Par Un Appendice Relatif Aux Fournitures d'eau de Plusieurs Villes Au Filtrage Des Eaux et a La Fabrication Des Tuyaux de Fonte, de Plomb, de Tole et de Bitume*. Victor Dalmont, Libraire des Corps

imperiaux des ponts et chaussées et des mines,. http://hdl.handle.net/2027/nyp.33433090927322.

Dershowitz, William Simon. 1984. "Rock Joint Systems." Thesis, Massachusetts Institute of Technology. https://dspace.mit.edu/handle/1721.1/27939.

Dershowitz, William Simon, and Hans H. Herda. 1992. "Interpretation of Fracture Spacing and Intensity." In . American Rock Mechanics Association. https://www.onepetro.org/conference-paper/ARMA-92-0757.

Dietrich, Peter, Rainer Helmig, Martin Sauter, Heinz Hötzl, Jürgen Köngeter, and Georg Teutsch, eds. 2005. *Flow and Transport in Fractured Porous Media*. Berlin/Heidelberg: Springer-Verlag. https://doi.org/10.1007/b138453.

Doe, T. W., and J. E. Geier. 1990. "Interpretation of Fracture System Geometry Using Well Test Data." STRIPA-TR--91-03. Swedish Nuclear Fuel and Waste Management Co. http://inis.iaea.org/Search/search.aspx?orig_q=RN:23001173.

Draganovic, Almir. 2009. "Bleeding and Filtration of Cement-Based Grout." http://urn.kb.se/resolve?urn=urn:nbn:se:kth:diva-11655.

Eklund, Daniel. 2005. "Penetrability Due to Filtration Tendency of Cement Based Grouts." http://urn.kb.se/resolve?urn=urn:nbn:se:kth:diva-200.

El Tani, Mohamed, and Håkan Stille. 2017. "Grout Spread and Injection Period of Silica Solution and Cement Mix in Rock Fractures." *Rock Mechanics and Rock Engineering* 50 (9): 2365–2380. https://doi.org/10.1007/s00603-017-1237-8.

Forman, Clemens, Ibrahim Kolawole Muritala, Robert Pardemann, and Bernd Meyer. 2016. "Estimating the Global Waste Heat Potential." *Renewable and Sustainable Energy Reviews* 57 (C): 1568–79.

Fransson, Åsa. 2002. "Nonparametric Method for Transmissivity Distributions Along Boreholes." *Groundwater* 40 (2): 201–4. https://doi.org/10.1111/j.1745-6584.2002.tb02505.x.

Fransson, Åsa . 2008. "Grouting Design Based on Characterization of the Fractured Rock Presentation and Demonstration of a Methodology." R-08-127. Svensk Kärnbränslehantering AB.

Fransson, Åsa, Johan Funehag, and Johan Thörn. 2016. "Swedish Grouting Design: Hydraulic Testing and Grout Selection." *Ground Improvement*, no. 4: 275–85. https://doi.org/10.1680/jgrim.15.00020.

Fransson, Åsa, and Gunnar Gustafson. 2006. "Efterinjektering: Inläckageprognos och design – förslag till analys." 75. SveBeFo.

Fransson, Åsa, and Gunnar Gustafson . 2007. "Efterinjektering - Förutsättningar Och Möjligheter." In . https://research.chalmers.se/en/publication/27096.

Funehag, Johan. 2007. "Grouting of Fractured Rock with Silica Sol; Grouting Design Based on Penetration Length." Chalmers University of Technology. https://research.chalmers.se/en/publication/25899.

Funehag, Johan. 2012. "GUIDE TO GROUTING WITH SILICA SOL - for Sealing in Hard Rock." 118. Stockholm: Stiftelsen för bergteknisk forskning.

Funehag, Johan. 2017. "Borrhål - Hydraulisk Gradient Och Erosion." 172. BeFo. http://www.befoonline.org/UserFiles/Archive/1123/BeFo_Rapport_172_webb.pdf.

Funehag, Johan, and Johan Claesson. 2017. "How the Pressure Build-Up Affects the Penetration Length of Grout-New Formulation of Radial Flow of Grout Incorporating Variable Pressure." In *Grouting 2017*, 143–51. Honolulu, Hawaii: American Society of Civil Engineers. https://doi.org/10.1061/9780784480793.014.

Funehag, Johan, and Ann Emmelin. 2011. "Injekteringen av TASS-tunneln – Design, genomförande och resultat från förinjekteringen." R-10-39.

Funehag, Johan, and Åsa Fransson. 2006. "Sealing Narrow Fractures with a Newtonian Fluid: Model Prediction for Grouting Verified by Field Study." *Tunnelling and Underground Space Technology* 21 (5): 492–98. https://doi.org/10.1016/j.tust.2005.08.010.

Funehag, Johan, and Gunnar Gustafson. 2005. "Grouting with Silica Sol in the Törnskog Tunnel, Grouting Design for Silica Sol in Full Production." https://research.chalmers.se/en/publication/8790.

Funehag, Johan, and Gunnar Gustafson. 2008a. "Design of Grouting with Silica Sol in Hard Rock – New Design Criteria Tested in the Field, Part II." *Tunnelling and Underground Space Technology* 23 (1): 9–17. https://doi.org/10.1016/j.tust.2006.12.004.

Funehag, Johan, and Gunnar Gustafson. 2008b. "Design of Grouting with Silica Sol in Hard Rock – New Methods for Calculation of Penetration Length, Part I." *Tunnelling and Underground Space Technology* 23 (1): 1–8. https://doi.org/10.1016/j.tust.2006.12.005.

Funehag, Johan, and Johan Thörn. 2018. "Radial Penetration of Cementitious Grout – Laboratory Verification of Grout Spread in a Fracture Model." *Tunnelling and Underground Space Technology* 72 (February): 228–32. https://doi.org/10.1016/j.tust.2017.11.020.

GeoERA. 2019. "Pilot Urban Areas in the MUSE Project." GeoERA. June 6, 2019. https://geoera.eu/projects/muse3/pilot-urban-areas-in-the-muse-project/.

Grandia, Fidel, Juan-Manuel Galíndez, David Arcos, and Jorge Molinero. 2010. "Quantitative Modelling of the Degradation Processes of Cement Grout – Project CEMMOD." TR-10-25. Svensk kärnbränslehantering AB SKB.

Grycz, David, Petr Hemza, and Zdeněk Rozehnal. 2014. "Charging of the Experimental High Temperature BTES Via CHP Unit - Early Results." *Energy Procedia*, Proceedings of the 2nd International Conference on Solar Heating and Cooling for Buildings and Industry (SHC 2013), 48 (January): 355–60. https://doi.org/10.1016/j.egypro.2014.02.041.

Gustafson, Gunnar. 2009. *Hydrogeologi För Bergbyggare*. Stockholm: Formas.

Gustafson, Gunnar, Johan Claesson, and Åsa Fransson. 2013. "Steering Parameters for Rock Grouting." Research article. Journal of Applied Mathematics. 2013. https://doi.org/10.1155/2013/269594.

Gustafson, Gunnar, and Åsa Fransson. 2005. "The Use of the Pareto Distribution for Fracture Transmissivity Assessment." *Hydrogeology Journal* 14 (1): 15–20. https://doi.org/10.1007/s10040-005-0440-y.

Gustafson, Gunnar, Åsa Fransson, Johan Funehag, and Magnus Axelsson. 2004. "Ett nytt angreppssätt för bergbeskrivning och analysprocess för injektering: geoteknik."

Gustafson, Gunnar, Magnus Hagström, and Zareen Abbas. 2008. "Beständighet av cementinjektering." Chalmers Tekniska Högskola.

Gustafson, Gunnar, and Håkan Stille. 2005. "Stop Criteria for Cement Grouting." *Felsbau : Zeitschrift Für Geomechanik Und Ingenieurgeologie Im Bauwesen Und Bergbau* 25:3, s. 62–68. http://urn.kb.se/resolve?urn=urn:nbn:se:kth:diva-64558.

Håkansson, Ulf. 1993. *Rheology of Fresh Cement-Based Grouts*. Trita-JOB 93:11. Stockholm: DissStockholm : Teknhögsk.

Holt, Erika. 2008. "Durability of Low-PH Injection Grout - A Literature Survey." 2007–57. Posiva. https://www.vtt.fi/inf/julkaisut/muut/2008/Posiva_WR2007-57.pdf.

Jones, Trevor A., and Russell L. Detwiler. 2016. "Fracture Sealing by Mineral Precipitation: The Role of Small-Scale Mineral Heterogeneity." *Geophysical Research Letters* 43 (14): 7564–71. https://doi.org/10.1002/2016GL069598.

Karasaki, K. 1986. “WELL TEST ANALYSIS IN FRACTURED MEDIA,” April. https://escholarship.org/uc/item/9tx2s07j.

Kobayashi, Shinji, and H\aakan Stille. 2007. “Design for Rock Grouting Basedon Analysis of Grout Penetration : Verification Using Äspö HRL Dataand Parameter Analysis.” In .

Kroehn, Klaus-Peter, and Bill Lanyon. 2018. “Observations of Hydraulic and Transport ‘“Skin Effects”’. SKB Task Force Workshop Praque 2016.” GRS--504. Gesellschaft fuer Anlagen- und Reaktorsicherheit (GRS) gGmbH. http://inis.iaea.org/Search/search.aspx?orig_q=RN:50020498.

Lindståhl, Henrik. 2018. “Spillvärmeförädling genom säsongsvärmelagring.” Stockholm. https://www.energiforetagen.se/globalassets/energiforetagen/det-erbjuder-vi/sakomraden/restvarmeseminarium/henrik-lindstahl.pdf.

Löfgren, Martin, and Ivars Neretnieks. 2003. “Formation Factor Logging by Electrical Methods. Comparison of Formation Factor Logs Obtained in Situ and in the Laboratory.” *Journal of Contaminant Hydrology* 61 (1–4): 107–15. https://doi.org/10.1016/S0169-7722(02)00117-1.

Lundström, Lars, and Håkan Stille. 1978. “Large Scale Permeability Test of the Granite in the Stripa Mine and Thermal Conductivity Test.” Stockholm, Sweden: Kärnbränslesäkerhet, KBS. https://escholarship.org/uc/item/5z64c1qp.

Mangold, Dick, and Laure Deschaintre. 2015. “Seasonal Thermal Energy Storage: Report on State of the Art and Necessary Further R+D.” IEA SHC Task 45. https://doi.org/10.18777/ieashc-task45-2015-0014.

Martinet, Philippe. 1998. “Flow and Clogging Mechanisms in Porous Media with Applications to Dams.” http://urn.kb.se/resolve?urn=urn:nbn:se:kth:diva-2607.

Mohammed, Mohammed Hatem, Roland Pusch, and Sven Knutsson. 2015. “Study of Cement-Grout Penetration into Fractures under Static and Oscillatory Conditions.” *Tunnelling and Underground Space Technology* 45 (January): 10–19. https://doi.org/10.1016/j.tust.2014.08.003.

Moye, D. G. 1967. “Diamond Drilling for Foundation Exploration.” *Civil Engineering Transactions* CE9 (1): 95–100.

Nordell, Bo. 1994. “Borehole Heat Store Design Optimization.” Luleå: Luleå University of Technology.

Nordell, Bo, Kent Fjällström, and L Öderyd. 1998. “WATER DRIVEN DOWN-THE-HOLE WELL DRILLING EQUIPMENT FOR HARD ROCK.”

Nordell, Bo, Alberto Liuzzo Scorpo, Olle Andersson, Leif Rydell, and Björn Carlsson. 2016. *Long-Term Long Term Evaluation of Operation and Design of the Emmaboda BTES. : Operation and Experiences 2010-2015*. Luleå tekniska universitet. http://urn.kb.se/resolve?urn=urn:nbn:se:ltu:diva-22591.

Nußbicker, J, D Mangold, W Heidemann, and H Müller-Steinhagen. 2003. “Solar Assisted District Heating System with Duct Heat Store in Neckarsulm-Amorbach (Germany).” In .

Olofsson, Bo, Gunnar Jacks, Gert Knutsson, and Roger Thunvik. 2001. “Grundvatten i Hårt Berg - En Analys Av Kunskapsläget.” In *SOU 2001:35 Kunskapsläget På Kärnavfallsområdet 2001*. https://www.karnavfallsradet.se/sites/default/files/documents/sou_2001_35_del_iii.pdf.

Paillet, F. L. 1994. *Application of Borehole Geophysics in the Characterization of Flow in Fractured Rocks*. U.S. Geological Survey.

Pan, Dongjiang, Nong Zhang, Chenghao Zhang, Deyu Qian, Changliang Han, and Sen Yang. 2018. “Long-Term Mechanical Behavior of Nano Silica Sol Grouting.” *Nanomaterials* 8 (1). https://doi.org/10.3390/nano8010046.

Piepho, M. G. 1997. "Long-Term Degradation (or Improvement?) Of Cementitious Grout/Concrete for Waste Disposal at Hanford." http://inis.iaea.org/Search/search.aspx?orig_q=RN:29041364.

Rahman, Mashuqur, and Ulf Håkansson. 2011. "IN-LINE RHEOLOGICAL MEASUREMENTS OF CEMENT BASED GROUTS USING THE UVP-PD METHOD." 99. BeFo. http://www.befoonline.org/UserFiles/Archive/243/Rapport_99.pdf.

Ranta-Korpi, Reeta, Petriikka Karttunen, and Ursula Sievänen. 2008. "R20 Programme: Field Testing of Grouting Materials." 2007–102. Posiva Oy. http://www.posiva.fi/files/463/WR_2007-102_web.pdf.

SGU Sveriges Geologiska Undersökning. n.d. "SGUs Kartvisare." Berggrund 1:50000 - 1:250000. Accessed December 19, 2019. https://apps.sgu.se/kartvisare/kartvisare-berg-50-250-tusen.html?zoom=387811.75843772915,6398768.462509355,645692.2741987607,6533168.731309893.

Sibbitt, Bruce, Doug McClenahan, Reda Djebbar, Jeff Thornton, Bill Wong, Jarrett Carriere, and John Kokko. 2012. "The Performance of a High Solar Fraction Seasonal Storage District Heating System – Five Years of Operation." *Energy Procedia* 30: 856–65. https://doi.org/10.1016/j.egypro.2012.11.097.

Skarphagen, Helge, David Banks, Bjørn S. Frengstad, and Harald Gether. 2019. "Design Considerations for Borehole Thermal Energy Storage (BTES): A Review with Emphasis on Convective Heat Transfer." Review Article. Geofluids. Hindawi. 2019. https://doi.org/10.1155/2019/4961781.

Smits, Alexander J. 2000. *A Physical Introduction to Fluid Mechanics*. New York: Wiley.

Snow, David Tunison. 1965. "A Parallel Plate Model of Fractured Permeable Media." Doctoral thesis, University of California, Berkeley.

Sögaard, Christian, Johan Funehag, and Zareen Abbas. 2018. "Silica Sol as Grouting Material: A Physio-Chemical Analysis." *Nano Convergence* 5 (February). https://doi.org/10.1186/s40580-018-0138-1.

Thörn, Johan, Sara Kvartsberg, Edward Runslätt, Sebastian Almfeldt, and Åsa Fransson. 2015. "Beräkningsverktyg För Bergkaraktärisering Vid Injekteringsdesign – Teori Och Användarhandledning." https://research.chalmers.se/en/publication/230208.

Tordrup, K. W., S. E. Poulsen, and H. Bjørn. 2017. "An Improved Method for Upscaling Borehole Thermal Energy Storage Using Inverse Finite Element Modelling." *Renewable Energy* 105 (May): 13–21. https://doi.org/10.1016/j.renene.2016.12.011.

Tuomas, Göran. 2004. "Water Powered Percussive Rock Drilling : Process Analysis, Modelling and Numerical Simulation." http://urn.kb.se/resolve?urn=urn:nbn:se:ltu:diva-26525.

U.S. Department of Energy. 2008. "Waste Heat Recovery: Technology and Opportunities in U.S. Industry." US Department of Energy.

Wahlgren, Carl-Henric, Claes Mellqvist, Kajsa Bovin, Cecilia Jelinek, Lena Persson, Bo Thunholm, and Hanna Wåhlén. 2015. "Grundvatten i kristallin berggrund, en pilotstudie baserad på SGUs data," 72.

Warner, James. 2004. *Practical Handbook of Grouting: Soil, Rock, and Structures*. John Wiley & Sons.

Williams, John H., and Carole D. Johnson. 2004. "Acoustic and Optical Borehole-Wall Imaging for Fractured-Rock Aquifer Studies." *Journal of Applied Geophysics*, Non-Petroleum Applications of Borehole Geophysics, 55 (1): 151–59. https://doi.org/10.1016/j.jappgeo.2003.06.009.

Zimmerman, Robert W. 2005. “Influence of Reynolds Number on Fluid Flow in Rock Fractures.” In . Stiftelsen svensk bergteknisk forskning, Svenska Bergmekanikgruppen.

IMPERMEABLE BOREHOLES FOR HIGH TEMPERATURE THERMAL ENERGY STORAGE

Waste heat is an inevitable by-product of every energy conversion process. Estimations show that around fifty percent of the global production of primary energy is wasted as exhaust or effluent losses, out of which approximately sixty percent are generated at temperature levels below 100 °C

The performance of a borehole thermal energy storage is highly dependent on the design of the heat exchangers used to provide heat exchange between the heat carrier and the rock. Development of new temperature-resistant borehole heat exchanger designs is an important step in accomplishing efficient storage of industrial surplus heat at high temperatures.

This pilot study has focused on investigating the application of permeation grouting techniques as a possible means of preventing or reducing fluid losses in open-hole pressurized boreholes. The study is a first step in the development of a novel type of coaxial borehole heat exchanger for high temperature borehole thermal energy storage applications in hard rock.

Energiforsk is the Swedish Energy Research Centre – an industrially owned body dedicated to meeting the common energy challenges faced by industries, authorities and society. Our vision is to be hub of Swedish energy research and our mission is to make the world of energy smarter!

Energiforsk